PULSE POLARIZATION ENTANGLED PHOTON GENERATED BY CHAOTIC SIGNALS IN A NONLINEAR MICRO RING RESONATOR FOR BIREFRINGENCE MEASUREMENT

PHUBET PHIPHITHIRANKARN

A THESIS SUBMITTED IN PARTIAL FULFILLMENT

OF THE REQUIREMENT FOR THE DEGREE OF

DOCTOR OF PHILOSOPHY IN APPLIED PHYSICS

FACULTY OF SCIENCE

KING MONGKUT'S INSTITUTE OF TECHNOLOGY LADKRABANG

2009

KMITL-2009-SC-D-030-017

หัวข้อวิทยานิพนธ์	การเกิดพัลซ์โพลาไรเซชันเอ็นแทงเกิลโฟตอนโดยสัญญาณไร้ระเบียบภายในนอนลิเนียร์ไมโครริงเรโซเนเตอร์สำหรับการวัดไบร์ฟรินเจนซ์
นักศึกษา	นายภูเบศร์ พิพิธหิรัญการ
รหัสประจำตัว	47063403
ปริญญา	ปรัชญาดุษฎีบัณฑิต
สาขาวิชา	ฟิสิกส์ประยุกต์
พ.ศ.	2552
อาจารย์ที่ปรึกษาวิทยานิพนธ์	รศ.ดร. ปรีชา ยุพาพิน

บทคัดย่อ

วิทยานิพนธ์ฉบับนี้นำเสนอแนวคิดการสร้างพัลซ์โพลาไรเซชันเอ็นแทงเกิลโฟตอนจากสัญญาณไร้ระเบียบที่เกิดภายในนอนลิเนียร์ไมโครริงเรโซเนเตอร์และอาศัยสมบัติความเป็นไบร์ฟรินเจนซ์เพื่อใช้ในการตรวจวัด หลักการคือการทำให้เกิดนอนลิเนียร์ภายในไมโครริงเรโซเนเตอร์โดยอาศัยปรากฏการณ์เคอร์ สัญญาณแสงที่เดินทางในนอนลิเนียร์ไมโครริงเรโซเนเตอร์จะกลายเป็นสัญญาณไร้ระเบียบที่เรียกว่าเคออส จากนั้นอาศัยปรากฏการณ์โฟร์เวฟมิกซิ่งและอุปกรณ์ควบคุมแนวโพลาไรซ์สร้างพัลซ์โพลาไรเซชันเอ็นแทนเกิลโฟตอนขึ้น ปกติคู่พัลซ์โพลาไรเซชันเอ็นแทนเกิลโฟตอนที่สร้างขึ้นจะมีแนวโพลาไรซ์ตั้งฉากซึ่งกันและกัน ดังนั้นถ้าไม่มีการรบกวนจากภายนอกแนวโพลาไรซ์ทั้งสองยังคงเดินทางคู่กันไปตลอด แต่ถ้าเกิดการรบกวนจากภายนอกเช่นเกิดความเค้นกับไมโครริงเรโซเนเตอร์จะทำให้เกิดปรากฏการณ์ไบร์ฟรินเจนซ์ขึ้นในไมโครริงเรโซเนเตอร์ ผลคือเกิดความต่างเฟสของคู่พัลซ์โพลาไรเซชันเอ็นแทนเกิลโฟตอน การหาความต่างเฟสทำได้โดยอาศัยกระบวนการชดเชยแบบวอล์คออฟ ดังนั้นถ้าหาความสัมพันธ์ระหว่างสิ่งที่รบกวนระบบกับความต่างเฟสของคู่พัลซ์โพลาไรเซชันเอ็นแทนเกิลโฟตอน ก็สามารถนำระบบที่นำเสนอนี้มาประยุกต์เป็นอุปกรณ์ตรวจวัดที่มีขนาดเล็กมากและมีความแม่นยำสูงได้ ซึ่งจะกล่าวในรายละเอียดต่อไป

Thesis Title	Pulse Polarization Entangled Photon Generated by Chaotic Signals in a Nonlinear Micro Ring Resonator for Birefringence Measurement
Student	Mr. Phubet Phiphithirankarn
Student ID	47063403
Degree	Doctor of Philosophy
Program	Applied Physics
Year	2009
Thesis Advisor	Assoc.Prof.Dr. Preecha Yupapin

ABSTRACT

This thesis proposes a new concept of birefringence based sensor using the entangled photon walk-off compensation. The superposition of nonlinear light known as four-wave mixing of the chaotic signals within a micro ring device is introduced by the Kerr nonlinear effects type. The possible two entangled photon pairs are randomly generated by using the external polarization control unit. Results obtained have shown that the entangled state walk-off of the pulse polarized photon within the ring device can be compensated. This means the changes in walk-off parameters, i.e. birefringence, of the ring resonator (sensing device) can be relatively measured to the changes in the applied physical parameters such as temperature, pressure, etc. The potential of using such a proposed system for birefringence based sensing application is plausible and discussed.

ACKNOWLEDGEMENTS

First, I would like to thank my advisor, Dr. Preecha Yupapin who has supported me thoughout my thesis with his patience, knowledge, and experience during to research at Advanced Research Center for Photonics (ARCP).

Second, I would like to thank specially all lecturers and instructors at department of applied physics, King Mongkut's institute of technology ladkrabang (KMITL) and department of physics, Srinakarinwirot university (SWU) for the education and the knowledge.

Third, I would like to thank my friends at ARCP and department of applied physics at KMITL for their conversation, discussion, advice, guidance, friendship and helpful everything.

Finally, for the greatest thank, I would like to thank my parents that are my father, my mother, and my sister for the supporting and the understanding me through my studies at the university. For special thank, I would like to thank the Yabosdee's family and Dr. Piyawadee Yabosdee for all their love.

Phubet Phiphithirankarn

CONTENTS

Pages

ABSTRACT IN THAI I

ABSTRACT IN ENGLISH II

ACKNOWLEDGEMENTS III

CONTENTS IV

LIST OF FIGURES VI

CHAPTER 1 INTRODUCTION 1

1.1 Statement and Significance of the Problems 1

1.2 Goal and Objective 2

1.3 Scope of the Thesis 2

CHAPTER 2 THEORETICAL BACKGROUND 3

2.1 Wave Equation in Optical Fibers 3

2.2 Nonlinear Pulse Propagation Equation.....4

2.3 Nonlinear Refraction 7

2.4 Optical Kerr Effect 8

2.5 Four-Wave Mixing 10

2.6 Principle of Nonlinear Birefringence 12

2.7 Conclusion 14

CHAPTER 3 NONLINEAR MICRO RING RESONATOR 15

3.1 Fiber Optic Ring Resonator.....15

3.2 Nonlinear Micro Ring Resonator 17

3.3 Optical Bistability, Bifurcation and Chaos.....18

3.4 Conclusion 22

CONTENTS (Cont.)

Pages

CHAPTER 4 PULSE POLARIZATION ENTANGLED PHOTON GENERATION 23

4.1 Entangled Photon Generation 23

4.2 Conclusion 30

CHAPTER 5 BIREFRINGENCE BASED SENSING APPLICATIONS 31

5.1 Birefringence Based Sensor 31

5.2 Walk-off Compensation 33

5.3 Conclusion 34

CHAPTER 6 CONCLUSION.....35

REFERENCES 37

APPENDIX 39

BIOGRAPHY 56

LIST OF FIGURES

Fig. Pages

3.1 The schematic diagram of a single ring resonator with a directional coupler.....15

3.2 The relationship between the normalized output intensity and the phase shift.....16

3.3 The diagrams of output power of NMRR, (a) the output power and number of roundtrips, (b) the output power and input power, both (a) and (b) are shown the nonlinear phenomenons that are optical bistability, optical bifurcation, and optical chaos.....19

3.4 The diagram of optical bistability and bifurcation of the input and output power relation with $\phi_0 = 0$, $\kappa = 0.9$, L = 80 m for various nonlinear refractive indices : (a) $n_2 = 2.2 \times 10^{-20}\ m^2W^{-1}$ and (b) $n_2 = 2.6 \times 10^{-20}\ m^2W^{-1}$.....20

3.5 The diagram of optical bistability and bifurcation of the input and output power relation with $n_2 = 3.2 \times 10^{-20}\ m^2W^{-1}$, $\kappa = 0.9$, and L = 80 m for various linear phase shifts : (a) $\phi_0 = \pi/4$, (b) $\phi_0 = \pi/2$, (c) $\phi_0 = 3\pi/4$, (d) $\phi_0 = \pi$.....21

4.1 Schematic diagram of a micro ring resonator with a coupling part of a micro ring resonator.....24

4.2 A schematic of the entangled photon generation and detection system ; PBS : Polarization Beam Splitter, D : Detectors.....26

4.3 The graphs of optical intensity of polarization entangled photon that is generated from NMRR with the phase difference, where (a) $\phi = 0^\circ$, (b) $\phi = 55^\circ$.....27

4.4 The polarization output of the chaotic signals with different coupling coefficients, where green (top) and blue (bottom) represent horizontal and vertical polarized lights, respectively (a) $\kappa = 0.02$, (b) $\kappa = 0$, (c) $\kappa = 0.2$ and (d) $\kappa = 0.3$.....28

4.5 The output of the chaotic signals, where various the coupling coefficients : (a) $\kappa = 0.3$, (b) $\kappa = 0.4$, (c) $\kappa = 0.5$ and (d) $\kappa = 0.7$.....29

5.1 A schematic of a nonlinear micro ring resonator for birefringence based sensor ; PBS : Polarization beam splitter.....31

5.2 The two orthogonal polarizations propagated with phase difference 0.35 radian.....32

CHAPTER 1

INTRODUCTION

1.1 Statement and Significance of the Problems

Yupapin [1] has shown a concept of an ultra high measurement resolution method using polarized photon in a fiber optic ring resonator. He has concluded that the shift in optimum entangled photon visibility can be compensated by the appropriate walk-off length, where the measurement resolution is increased by the order of the change in material birefringence. However, the structure of fiber optic system becomes a problem due to the external environment suffering. Alternatively, an optical micro ring resonator has been widely investigated both theoretical and experimental works. It is found that the device scale is dramatically decreased, where the device scale of few microns is fabricated and available [2]. One of the promising application aspects is that it can be fabricated to process the signal processing within the small device, where the secure message, i.e. security, can be performed. For instance, the techniques such as chaos [3,4], quantum entanglement [5,6] and chaotic quantum [7] have shown the potential of applications. Recently, Fietz and Shvets [8] have reported that the polarized entangled photons can be generated by using a micro ring device, which is associated with the practical devices which have been fabricated. Yupapin [9] have shown that the entangled photon recovery i.e. regeneration using fiber optic ring resonator incorporating an EDFA which is useful for long distance link. However, the problem of polarization dispersion causes the entangled photon a problem called timing walk-off, which is become a problem in the recovery process. In this paper, we design the micro ring device to generate the polarized entangled photons for sensing applications. The entangled photon generation and behaviors within the proposed device is analyzed and discussed. The device parameters are simulated associating to the practical device. Results obtained have shown that it is a good potential of using such a device for birefringence based sensing applications, where the measurement of physical parameters such as temperature, pressure, moisture is plausible. The ultra high resolution in term of walk-off length and material birefringence is described.

1.2 Goal and Objective

The objectives of thesis are a study of the generation and sensing applications of polarization entangled photon by using nonlinear micro ring resonator. This polarization entangled photon is used for birefringence based sensing applications. The used principle is the changes of birefringence of polarization entangled photon by the applied physical parameters such as strain, temperature, force, pressure, etc. Then the relationship between the applied physical parameter and the occurred birefringence are used for the sensing applications based on birefringence.

1.3 Scope of the Thesis

The pulse polarization entangled photon is generated by a nonlinear micro ring resonator. The nonlinear effects within a micro ring resonator are optical Kerr effect and four wave mixing. The orthogonal polarization of entangled photon are measured by using the rotatable polarizer, polarization beam splitter, and two detectors. The applied physical parameter is the external strain perturbation, causing the birefringence to occur. The relationship between the applied physical parameter and birefringence are used for birefringence based sensing applications. All results have shown in this thesis, using the mathematical model and the simulation.

CHAPTER 2

THEORETICAL BACKGROUND

2.1 Wave Equation in Optical Fibers

From Maxwell's equations, these equations can be used to derive the wave equation that describes light propagation in optical fibers. In general, the wave equations can be written in favor of electric field (E) and induced polarization (P) as

$$\nabla \times \nabla \times E = -\frac{1}{c^2}\frac{\partial^2 E}{\partial t^2} - \mu_0 \frac{\partial^2 P}{\partial t^2} \tag{2.1}$$

Where c is the speed of light in vacuum and $\mu_0 \varepsilon_0 = 1/c^2$. In general, the evaluation of P requires a quantum-mechanical approach. The interesting case of light propagation in optical fibers is the study of nonlinear effects. If we include only the third-order nonlinear effects governed by $\chi^{(3)}$, the induced polarization consists of two parts such that

$$P(r,t) = P_L(r,t) + P_{NL}(r,t) \tag{2.2}$$

Where the linear part P_L and the nonlinear part P_{NL} are related to the electric field by

$$P_L(r,t) = \varepsilon_0 \int_{-\infty}^{\infty} \chi^{(1)}(t-t') \cdot E(r,t')dt' \tag{2.3}$$

$$P_{NL}(r,t) = \varepsilon_0 \iint_{-\infty}^{\infty} \chi^{(3)}(t-t_1, t-t_2, t-t_3) \cdot E(r,t_1)E(r,t_2)E(r,t_3)dt_1 dt_2 dt_3 \tag{2.4}$$

Eq. (2.1)-(2.4) provide a general formalism for studying the third-order nonlinear effects in optical fibers. In a major simplification, the nonlinear polarization P_{NL} in Eq. (2.2) is treated as a small perturbation to the total induced polarization. This is justified because the nonlinear effects are relatively weak in silica fibers. Therefore Eq. (2.1) with $P_{NL} = 0$ can be rewritten in the frequency domain and the refractive index (n) of optical fibers as

$$\nabla^2 E + n^2(\omega)\frac{\omega^2}{c^2}E = 0 \tag{2.5}$$

2.2 Nonlinear Pulse Propagation Equation

The study of most nonlinear effects in optical fibers involves the use of short pulses with widths ranging from about 10 ns to 10 fs. When optical pulses propagate inside a optical fibers, both dispersive and nonlinear effects influence their shape and wavelength. A basic equation that governs propagation of optical pulses in nonlinear dispersive fibers, it can be written in the form

$$\nabla^2 E - \frac{1}{c^2}\frac{\partial^2 E}{\partial t^2} = \mu_0\left(\frac{\partial^2 P_L}{\partial t^2} + \frac{\partial^2 P_{NL}}{\partial t^2}\right) \tag{2.6}$$

To solve of Eq. (2.4), firstly P_{NL} is treated as a small perturbation to P_L. This is justified because nonlinear changes in the refractive index are less than 10^{-6} in practice. Second, the optical field is assumed to maintain its polarization along the fiber length so that a scalar approach is valid. Third, the optical field is assumed to be quasi-monochromatic that the centered pulse spectrum is ω_0 and a spectral width $\Delta\omega$ such that $\Delta\omega/\omega_0 << 1$. Since $\omega_0 \approx 10^{15} s^{-1}$, the last assumption is valid for pulses as short as 0.1 ps. In the slowly varying envelope approximation adopted here, it is useful to separate the rapidly varying part of the electric field by writing it in the form

$$E(r,t) = \frac{1}{2}\hat{x}[E(r,t)\exp(-i\omega_0 t) + c.c.] \tag{2.7}$$

Where $\hat{x}$ is the unit vector of polarization, and $E(r,t)$ is a slowly varying function of time. The polarization components P_L and P_{NL} can be expressed in a similar way by

$$P_L(r,t) = \frac{1}{2}\hat{x}[P_L(r,t)\exp(-i\omega_0 t) + c.c.] \tag{2.8}$$

$$P_{NL}(r,t) = \frac{1}{2}\hat{x}[P_{NL}(r,t)\exp(-i\omega_0 t) + c.c.] \tag{2.9}$$

The linear component P_L is given by

$$P_L(r,t) = \varepsilon_0 \int_{-\infty}^{\infty} \chi^{(1)}(t-t') \cdot E(r,t') \exp[i\omega_0(t-t')]dt' \tag{2.10}$$

Or, to rewrite in the frequency domain is

$$P_L(r,t) = \frac{\varepsilon_0}{2\pi} \int_{-\infty}^{\infty} \chi^{(1)}(\omega) \cdot E(r,\omega-\omega_0) \exp[-i(\omega-\omega_0)t]d\omega \tag{2.11}$$

If the nonlinear response is assumed to be instantaneous so that the time dependence of $\chi^{(3)}$ in Eq. (2.4) is given by

$$P_{NL}(r,t) = \varepsilon_0 \chi^{(3)} \cdot E(r,t) \cdot E(r,t) \cdot E(r,t) \tag{2.12}$$

From Eq. (2.7) and Eq. (2.12), P_{NL} is found to have a term oscillating at ω_0 and another term oscillating at the third-harmonic frequency $3\omega_0$. The latter term requires phase matching and is generally negligible in optical fibers. Thus, P_{NL} is given by

$$P_{NL}(r,t) \approx \varepsilon_0 \varepsilon_{NL} E(r,t) \tag{2.13}$$

Where the nonlinear contribution to the dielectric constant is defined as

$$\varepsilon_{NL} = \frac{3}{4} \chi^{(3)} |E(r,t)|^2 \tag{2.14}$$

Thus, the general dielectric constant with nonlinear effects is given by

$$\varepsilon(\omega) = 1 + \chi^{(1)}(\omega) + \varepsilon_{NL} \tag{2.15}$$

The dielectric constant can be used to define the refractive index n and n become intensity dependent because of ε_{NL} by

$$n = n_0 + n_2 |E|^2 \tag{2.16}$$

Where n_2 is the nonlinear index coefficient that is given by

$$n_2 = \frac{3}{8n}\chi^{(3)} \tag{2.17}$$

The general form of the nonlinear wave propagation equation $A(r,t)$ for the slowly varying amplitude $E(r,t)$ and all the perturbation effects, such as the nonlinear effects, optical fiber losses, and dispersion, can be given by

$$\frac{\partial A}{\partial z} + \beta_1 \frac{\partial A}{\partial t} + \frac{i\beta_2}{2}\frac{\partial^2 A}{\partial^2 t} + \frac{\alpha}{2}A = i\gamma |A|^2 A \tag{2.18}$$

Where the nonlinear parameter γ is defined as

$$\gamma = \frac{n_2 \omega_0}{cA_{eff}} \tag{2.19}$$

Where A_{eff} is the effective core area. From Eq. (2.18), the pulse amplitude A is assumed to be normalized such that $|A|^2$ represents the optical power. The quantity $\gamma|A|^2$ is then measured in units of m^{-1} if n_2 is expressed in units of m^2/W. Clearly A_{eff} depends on fiber parameters such as the core radius and the core-cladding index difference. Typically, A_{eff} can vary in the range 20-100 μm^2 in the 1.5 μm region depending on the fiber design. As a result, γ takes values in the range 1-10 W^{-1}/km if $n_2 \approx 2.6\times10^{-20} m^2/W$. In a large effective area fiber, A_{eff} is increased intentionally to reduce the impact of fiber nonlinearity. From Eq. (2.18) describes propagation of optical pulse in single mode fibers. It is called the nonlinear Schrodinger (NLS) equation. In the equation, it includes the effects of fiber losses through α, chromatic dispersion through β_1 and β_2 , and fiber nonlinearity throught γ. The physical significance of β_1 and β_2 has been described that the pulse envelope moves at the group velocity $v_g = 1/\beta_1$ while the effects of group-velocity dispersion (GVD) are governed by β_2. The GVD parameter β_2 can be positive or negative depending on the wavelength λ is below or above the zero-dispersion wavelength λ_D of the fiber. In the anomalous-dispersion regime $(\lambda > \lambda_D)$, β_2 is

negative, and the fiber can support optical solitons. In standard silica fibers, $\beta_2 \sim 50\ ps^2/km$ in the visible region but becomes close $\sim 20\ ps^2/km$ near wavelength $\sim 1.5\ \mu m$, the change in sign occurring in the vicinity of $1.3\ \mu m$.

2.3 Nonlinear Refraction

The lowest-order nonlinear effects in optical fibers originate from the third-order susceptibility $\chi^{(3)}$, which is responsible form phenomena such as third-harmonic generation, four-wave mixing, and nonlinear refraction. Unless special efforts are made to achieve phase matching, the nonlinear processes that involve generation of new frequencies (e.g. third-harmonic generation and four-wave mixing) are not efficient in optical fibers. Most of the nonlinear effects in optical fibers therefore originate from nonlinear refraction, a phenomenon referring to the intensity dependence of the refractive index that can be written as

$$n = n(\omega) + n_2 |E|^2 \tag{2.20}$$

Where $n(\omega)$ is the linear part that is the refractive index of the medium resonances, in general, depends on the optical frequency (ω). The second term, $|E|^2$ is the optical intensity inside the optical fibers, and n_2 is the nonlinear index coefficient related to $\chi^{(3)}$ by

$$n_2 = \frac{3}{8n_0}\chi^{(3)} \tag{2.21}$$

Where the optical filed is assumed to be linearly polarized so that only one component $\chi^{(3)}$ contributes to the refractive index. The nature of $\chi^{(3)}$ can affect the polarization properties of optical filed through nonlinear birefringence.

The intensity dependence of the refractive index leads to the two most widely studied of interesting nonlinear effects that are self-phase modulation (SPM) and cross-phase modulation (XPM). Self-phase modulation refers to the self-induced phase shift experienced by an optical field during its propagation in optical fibers. Its magnitude can be obtained by

$$\phi = nk_0L = (n + n_2 |E|^2)k_0L \tag{2.22}$$

Where $k_0 = 2\pi/\lambda$ and L is the fiber length. The intensity dependent nonlinear phase shift $\phi_{NL} = n_2 k_0 L |E|^2$ is due to SPM. SPM is responsible for spectral broadening of ultrashort pulses and formation of optical solitons in the anomalous dispersion regime of optical fibers.

Cross-phase modulation refers to the nonlinear phase shift of an optical field induced by another field having a different wavelength, direction, or state of polarization. If the electric field is given by

$$E = \frac{1}{2}\hat{x}[E_1 \exp(-i\omega_1 t) + E_2 \exp(-i\omega_2 t) + c.c.] \tag{2.23}$$

When two optical fields at frequencies ω_1 and ω_2, polarized along the x-axis, propagate simultaneously inside the optical fibers (the abbreviation c.c. stands for complex conjugate). The nonlinear phase shift for the field at ω_1 is given by

$$\phi_{NL} = n_2 k_0 L(|E_1|^2 + 2|E_2|^2) \tag{2.24}$$

Where we have neglected all terms that generate polarization at frequencies other than ω_1 and ω_2 because of their non-phase matched character. The two terms on the right hand are SPM and XPM, respectively. An important feature of XPM is that, for equally intense optical fields of different wavelengths, the contribution of XPM to the nonlinear phase shift is twice that of SPM and XPM is responsible for asymmetric spectral broadening of co-propagating optical pulses.

2.4 Optical Kerr Effect

The optical Kerr effect is a change in the refractive index of a material, depending on an electric field. The changes of refractive index is directly proportional to the square of the electric field. For a nonlinear material, the electric polarization field P depends on the electric field E by

$$P = \varepsilon_0 \chi^{(1)} E + \left(\varepsilon_0 \chi^{(2)} E \cdot E + \varepsilon_0 \chi^{(3)} E \cdot E \cdot E + \ldots\right) = P_L + P_{NL} \tag{2.25}$$

Where ε_0 is the vacuum permittivity and $\chi^{(n)}$ is the n^{th} order component of the electric susceptibility of the medium. For a linear medium, only the first term of this equation is significant and the linear polarization (P_L) varies linearly with the electric field. The second and higher order

terms are represented the nonlinear polarization (P_{NL}). For the second-order susceptibility $\chi^{(2)}$ vanishes for an isotropic medium such as silica (SiO_2) that is a symmetric molecule, resulting the second order susceptibility is approximately equal to zero. Thus all nonlinear effects in optical fibers are determined by the third order susceptibility $\chi^{(3)}$.

To consider, the equation of electric field in a medium is $E = E_0 \cos(\omega t)$ where E_0 is the amplitude. Thus the equation of polarization with the nonlinear terms $\varepsilon_0 \chi^{(3)} |E_0|^3$ is given by

$$P \approx \varepsilon_0 \left(\chi^{(1)} + \frac{3}{4} \chi^{(3)} |E_0|^2 \right) E_0 \cos(\omega t) \tag{2.26}$$

The linear susceptibility with an additional nonlinear term can be assigned by

$$\chi = \chi_L + \chi_{NL} = \chi^{(1)} + \frac{3}{4} \chi^{(3)} |E_0|^2 \tag{2.27}$$

And

$$n = (1+\chi)^{1/2} = (1 + \chi_L + \chi_{NL})^{1/2} \approx n_0 \left(1 + \frac{1}{2n_0^2} \chi_{NL} \right) \tag{2.28}$$

Where $n_0 = (1+\chi_L)^{1/2}$ is the linear refractive index of the material. Using a Taylor expansion and approximation $\chi_{NL} << (1+\chi_L)$, thus the refractive index depends on the intensity is

$$n = n_0 + \frac{3}{8n_0} \chi^{(3)} |E_0|^2 = n_0 + n_2 I \tag{2.29}$$

Where I is the intensity of light. n_2 is the nonlinear refractive index known as the Kerr coefficient, it has very small value for most materials, $n_2 \approx 3.2 \times 10^{-20}\ m^2/W$ for silica fibers. Thus the refractive index change is directly proportional to the intensity of light travelling through the medium. The value of intensity can be produced the significant variations of nonlinear refractive index about $1\ GW\ cm^{-2}$.

For a single-mode silica fiber, the nonlinear refractive index can be rewritten into the input power (P) that is given by

$$n = n_0 + \frac{n_2 P}{A_{eff}} \tag{2.30}$$

Where $A_{eff} = 50\ \mu m^2$ is an effective area of single-mode fiber core.

2.5 Four-Wave Mixing

Four-wave mixing (FWM) is a process which light at frequencies ω_1 and ω_2 interact in a nonlinear material that means the nonlinear susceptibility $\chi^{(3)}$ to create an output light at frequency ω_3 and ω_4 satisfying a phase relationship that is called "phase matching condition". Because of the second order susceptibility $\chi^{(2)}$ is neglected for the silica fiber. The third order susceptibility is considered for FWM.

In quantum mechanic representation that different photons annihilate to generate new ones at different frequency such that the net energy and momentum are conserved during the parametric interaction. The different kinds of FWM are possible. The case in which three photons annihilate to give rise to a new one ($\omega_1 + \omega_2 + \omega_3 = \omega_4$), is called "totally degenerate FWM". The case of two photons annihilate to give rise to two photons different frequency ($\omega_1 + \omega_2 = \omega_3 + \omega_4$), is called "partially degenerate FWM". Finally the "non-degenerate FWM" is presented when all frequencies are difference.

The equations constitutes the phase matching condition and frequency matching condition for FWM are shown in Eq. (2.31) and (2.32), respectively.

$$k_1 + k_2 = k_3 + k_4 \tag{2.31}$$

$$\omega_1 + \omega_2 = \omega_3 + \omega_4 \tag{2.32}$$

Where ω_1 and ω_2 are the frequencies of two input photons; ω_3 and ω_4 are the frequencies of two output photons from the annihilation of FWM process. For the partially degenerate case the phase matching condition for all photons is satisfied by

$$\Delta k = k_1 + k_2 - k_3 - k_4 = 0 \tag{2.33}$$

Where $k(\omega)$ is the propagation constant for the light with frequency ω. It's easy to satisfy $\Delta k = 0$ in the specific case $\omega_1 = \omega_2$ that called partially FWM. This case is most relevant for optical fibers. Physically, a pump photons at frequency ω_1 creates two sidebands located symmetrically at frequencies ω_3 and ω_4 with a frequency shift (Ω_S)

$$\Omega_S = \omega_1 - \omega_3 = \omega_4 - \omega_1 \tag{2.34}$$

The phase matching depends on the dopant, the doping concentration, the refractive index difference, and the diameter of fiber core.

In the partially FWM, two photons at a pump frequency (ω_p) are absorbed by the optical fiber and two photons are created. One photon has a higher frequency (ω_{AS}) than the pump frequency and one photon at a lower frequency (ω_S). Usually high frequency and low frequency are referred as anti-Stokes and Stokes photon, respectively. Normally, the Stokes and anti-Stokes are called the signal and idler photons. Sometime this case is call Three-wave mixing.

$$\omega_P + \omega_P = \omega_S + \omega_{AS} \tag{2.35}$$

For single mode fiber both the material and waveguide dispersions contribute by

$$\Delta k = 2\beta_2(\Delta\omega)^2 \tag{2.36}$$

Where $\beta_n = \partial^n\beta / \partial\omega^n$ is the group velocity dispersion (GVD). When $\beta_2 = 0$, it's a perfect phase matching and an efficient FWM. This situation is desirable for applications such as all-optical signal processing, wavelength conversion, pulse compression , etc. FWM in optical fibers can be used for generating spectrally inverted signal through the process of optical phase conjugation (OPC), which is useful for dispersion compensation. However, in WDM systems FWM causes a transfer of power from each channel to its neighbors. Such a power transfer not only results in the power loss for the channel but also induces interchannel crosstalk that degrades the system performance severely. This problem can be minimized using the technique of dispersion management, in which the fiber dispersion is kept locally high even though it is low on

average. Non-zero dispersion shifted fibers have been developed with a finite but small dispersion (~ 2 to 8 ps/km) in order to reduce FWM effects in actual fiber optic communication systems.

2.6 Principle of Nonlinear Birefringence

Normally, a single-mode fiber supports two orthogonally polarized mode with the same spatial distribution and this two modes are degenerated in an ideal fiber that their effective refractive indices, n_x and n_y are identical. In practice, all fibers exhibit some modal birefringence ($n_x \neq n_y$) because of unintentional variations in the core shape and anisotropic stresses along the fiber length. If nearly constant birefringence along their entire length, this kind of birefringence is call "linear birefringence". However, if a sufficiently intense light are launched into optical fiber, the nonlinear birefringence can be induced where amplitude is intensity dependent.

An optical fiber with constant modal birefringence has two principal axes which the fiber is capable of maintaining the state of linear polarization of the incident light. Two principle axes are called slow and fast axes based on the speed of light that travels inside the fiber. If $n_x > n_y$, thus n_x is the mode along fast axis. When low-power light is launched with its polarization direction oriented at an angle with respect to the fast or slow axes, the polarization state changes along the fiber axes from linear to elliptic, elliptic to circular, and finally back to linear in a period. The distance satisfies with a periodic of polarization change, called beat length.

Considering the electric field with arbitrary polarization along the principal axes, can be written as

$$\vec{E}(\vec{r},t) = (\hat{x}E_x + \hat{y}E_y)\exp(-i\omega_0 t) \tag{2.37}$$

Where E_x and E_y are the amplitudes of the polarization components along the x-axis and y-axis, respectively. ω_0 is the carrier frequency. From third order susceptibility ($\chi^{(3)}$), the nonlinear polarization (P_{NL}) can be written as

$$\vec{P}_{NL}(\vec{r},t) = (\hat{x}P_x + \hat{y}P_y)\exp(-i\omega_0 t) \tag{2.38}$$

Where

$$P_x = \frac{3\varepsilon_0}{4}\chi^{(3)}\left[\left(|E_x|^2 + \frac{2}{3}|E_y|^2\right)E_x + \frac{1}{3}\left(E_x^* E_y\right)E_y\right] \tag{2.39}$$

And

$$P_y = \frac{3\varepsilon_0}{4}\chi^{(3)}\left[\left(|E_y|^2 + \frac{2}{3}|E_x|^2\right)E_y + \frac{1}{3}\left(E_y^* E_x\right)E_x\right] \tag{2.40}$$

The last term in Eq. (2.39) and (2.40) leads to degenerate four-wave mixing. The nonlinear contribution Δn_x to the refractive index is governed by the term proportional to E_x and otherwise. Then the nonlinear contributions Δn_x and Δn_y are given by

$$\Delta n_x = n_2\left(|E_x|^2 + \frac{2}{3}|E_y|^2\right) \tag{2.41}$$

And

$$\Delta n_y = n_2\left(|E_y|^2 + \frac{2}{3}|E_x|^2\right) \tag{2.42}$$

Where n_2 is the nonlinear refractive index or Kerr coefficient. From Eq. (2.41) and (2.42), the first term is responsible for self-phase modulation (SPM) and the second term result in cross-phase modulation (XPM) because the nonlinear phase shift acquired by one polarization component depends on the intensity of the other polarization component. The nonlinear contributions Δn_x and Δn_y are in general unequal and create nonlinear birefringence whose amplitude depends on the intensity and the polarization state of the incident light. In the case of light propagating inside a optical fiber, nonlinear birefringence manifests as a rotation of the polarization ellipse.

2.7 Conclusion

First, this chapter describes the wave equation in optical fibers by using Maxwell's equation. Second, describes the nonlinear effects in optical fibers for the nonlinear pulse propagation equation. This part describes the third-order susceptibility, nonlinear refractive index and nonlinear Schrodinger equation (NLS). Then, shows the nonlinear refraction depending on the light intensity and referred to SPM and XPM. Third, describes the optical Kerr effect occurred from the intensity of electric field. After that, explains the FWM creating an output light at frequency ω_3 and ω_4 from input light at frequency ω_1 and ω_2 by using nonlinear susceptibility $\chi^{(3)}$. Finally, describes the nonlinear birefringence that is occurred from the unequal of the effective refractive indices, n_x and n_y along the principal axes of the optical fibers. This is caused the slow and fast axes of the speed of light that travels inside the fiber. Besides, if a sufficiently intense light are launched into optical fiber, the nonlinear birefringence can be induced where amplitude is intensity dependent.

CHAPTER 3

NONLINEAR MICRO RING RESONATOR

3.1 Fiber Optic Ring Resonator (FORR)

A fiber optic ring resonators (FORR) is a closed loop waveguide that consists of a input port and a output port associated with a directional coupler through a piece of fiber to form a ring. The most feature of FORR is a two-ports device and light propagates only in the forward direction. When light of the appropriate wavelength is launched into a ring resonator, it builds up the intensity over multiple round trips due to constructive and destructive interference and stores the light at the resonance frequencies that determined by its specifications. From the properties of resonator, only some wavelengths is resonated in a loop, it is the functions of filter. The simple model of a FORR with radius R and circumference L, is shown in Fig. 3.1.

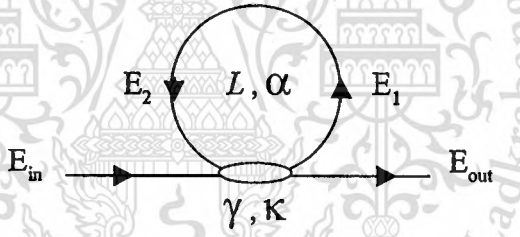

Fig. 3.1 The schematic diagram of a single ring resonator with a directional coupler.

Where κ is the coupling coefficient, α is the intensity attenuation coefficient, and γ is the intensity insertion loss coefficient of the directional coupler. When the monochromatic light is launched into a single ring resonator, the normalized output intensity from a output port can be derived as follows

$$E_{out} = \sqrt{1-\gamma}\left(E_{in}\sqrt{1-\kappa} + iE_2\sqrt{\kappa}\right) \tag{3.1}$$

$$E_1 = \sqrt{1-\gamma}\left(iE_{in}\sqrt{\kappa} + E_2\sqrt{1-\kappa}\right) \tag{3.2}$$

$$E_2 = E_1 \exp\left(-\frac{\alpha L}{2} - ikL\right) \tag{3.3}$$

Where $k = 2\pi n / \lambda$ is the wave propagation constant, n is the refractive index of fiber core. To used Eqs. (3.1) to (3.3) derived the normalized output intensity that is given by

$$\left|\frac{E_{out}}{E_{in}}\right|^2 = (1-\gamma)\left[1 - \frac{\kappa\left(1-(1-\gamma)e^{-\alpha L}\right)}{\left(1-e^{-\alpha L/2}\sqrt{(1-\gamma)(1-\kappa)}\right)^2 + 4e^{-\alpha L/2}\sqrt{(1-\gamma)(1-\kappa)}\sin^2(\phi/2)}\right] \tag{3.4}$$

Where $\phi = kL$ is linear phase shift. The normalized output intensity of a single ring resonator is shown in Fig. 3.2.

Fig. 3.2 The relationship between the normalized output intensity and the phase shift.

The parameters of the numerical results in Fig. 3.2 are λ = 1.55 μm, n = 1.45, κ = 0.1, γ = 0.15, α = 0.02 dB/km, and R = 100 μm. From Eq. (3.4) and Fig. 3.2, a FORR can be used for the sensing applications by using the relationship between the phase shift and the applied physical parameters that are applied on a FORR. The applied parameters such as strain, temperature, force and pressure etc. Besides that the phase shift may be depends on the refractive index of fiber core, the wavelength of light, and the radius of a FORR.

3.2 Nonlinear Micro Ring Resonator (NMRR)

A schematic diagram of nonlinear micro ring resonator (NMRR) is shown in Fig. 3.1, when the monochromatic light with amplitude E_0 and a random phase ϕ are launched into a NMRR. The input light (E_{in}) can be expressed as

$$E_{in} = E_0 e^{j\phi} \tag{3.5}$$

Because the refractive index depends on the intensity of light, the phase shift of light during its propagation in optical fibers can be obtained by

$$\phi = \phi_L + \phi_{NL} = nkL \tag{3.6}$$

Where $\phi_L = n_0 kL$ is the linear phase shift, $\phi_{NL} = n_2 kL\,|E|^2$ is the nonlinear phase shift depending on the intensity, L is the fiber length, and $k = 2\pi/\lambda$ is the wave propagation constant. If we assume that the only considered nonlinear is a Kerr effect, the refractive index of NMRR is given by

$$n = n_0 + n_2 I = n_0 + \left(\frac{n_2}{A_{eff}}\right)P \tag{3.7}$$

where n_0 and n_2 are the linear and the nonlinear refractive indices, respectively. I and P are the optical intensity and the optical power, respectively. The effective core area of a micro ring resonator is A_{eff}, which is in the range 0.12-0.50 μm^2.

From Eq. (3.4)-(3.7), the general equation of normalized output intensity of NMRR can be expressed by

$$\left|\frac{E_{out}}{E_{in}}\right|^2 = (1-\gamma)\left[1 - \frac{\kappa - \kappa(1-\gamma)x^2}{\left(1 - x\sqrt{(1-\gamma)(1-\kappa)}\right)^2 + 4x\sqrt{(1-\gamma)(1-\kappa)}\sin^2(\phi/2)}\right] \tag{3.8}$$

Where $x = \exp(-\alpha L/2)$ represents a round-trip losses coefficient, κ is the coupling coefficient, α is the intensity attenuation coefficient, γ is the intensity insertion loss coefficient.

3.3 Optical Bistability, Bifurcation, and Chaos

The optical bistability is the nonlinear phenomenon that occurred in optical devices where two resonant transmissions states are possible and stable, dependent on the input power or light intensity. This phenomenon is found in the optical devices with a feedback mechanism such as laser cavity, optical resonator, etc., providing two methods of achieving bistability. First, Absorptive bistability utilizes an absorber to block light inversely dependent on the intensity of the source light. The first bistable state resides at a given intensity where no absorber is used. The second state resides at the point where the light intensity overcomes the absorber's ability to block light. Second, refractive bistability utilizes an optical mechanism that changes its refractive index inversely dependent on the intensity of the source light. The first bistable state resides at a given intensity where no optical mechanism is used. The second state resides at the point where a certain light intensity causes the light to resonate to the corresponding refractive index. This effect is caused by two factors that are nonlinear atom-field interaction and feedback effect of mirror. The Applications of this phenomenon include its use in optical transmitters, memory elements and pulse shapers.

The optical bistability has been studied in non-fiber resonators since 1976 by placing the nonlinear medium inside a cavity formed by using multiple mirrors [11-13]. The single mode fiber is used in 1983 by using nonlinear medium inside a ring cavity [14]. Eqs. (3.5)-(3.8) are mathematical relations used for characterizing nonlinear effects such as optical bifurcation, optical bistability, and optical chaos.

From Eq. (3.8), the parameters is used to simulate the nonlinear phenomenons in the NMRR are $\lambda_0 = 1.55$ μm, $n_0 = 3.37$, $n_2 = 2.69 \times 10^{-17}$ m^2W^{-1}, $\alpha = 0.2$ dB/km, $\gamma = 0.01$, R = 100 μm, $\kappa = 0.2$, $\phi_0 = 0$ for simplicity, and the data of 10,000 iterations of round trips inside the NMRR is plotted. The results of mathematical method are shown in Fig. (3.2).

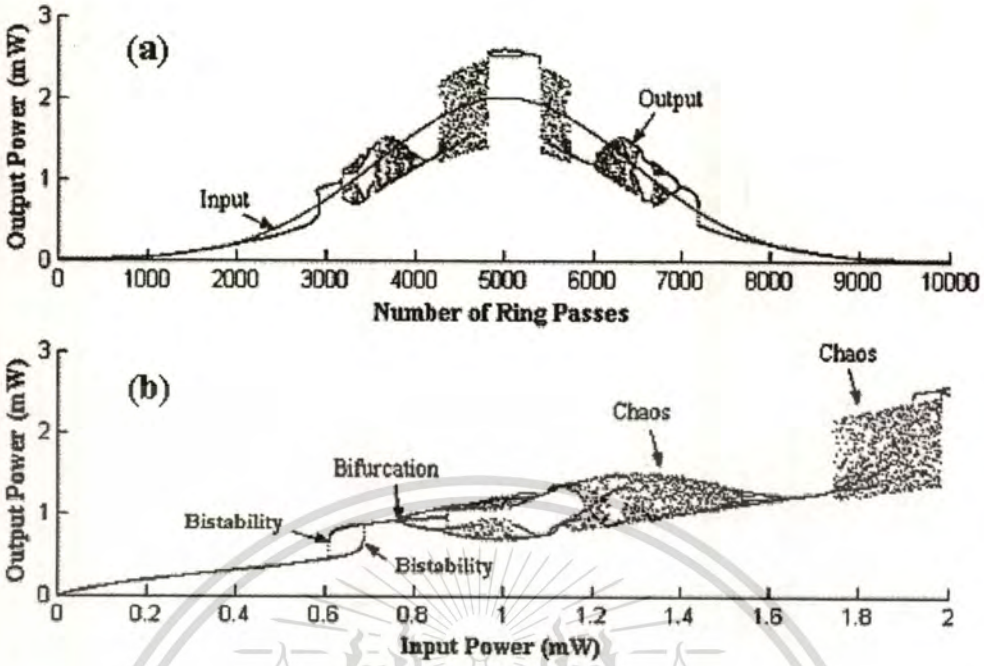

Fig. 3.3 The diagrams of output power of NMRR, (a) the output power and number of roundtrips, (b) the output power and input power, both (a) and (b) are shown the nonlinear phenomenons that are optical bistability, optical bifurcation, and optical chaos.

In Fig. 3.3(a) shows the nonlinear diagram of output power versus the CW input power. The bistability occurs in the range of input power 0.6069-0.6894 mW (the round trips at 2928) and the bifurcation appears when the input power is ranged between 0.7513-0.8484 mW (the round trips at 3168). Then the optical chaos occurs when the input power increasing than 0.8484 mW and maximum at 1.6494 mW. When the CW pulse trains circulated along the NMRR, the self-phase modulation of light induced the interference while propagating along the resonator which results the bifurcation, which is lead to the optical chaos. The chaotic behaviors of light traveling along the NMRR caused the change of $\chi^{(3)}$ which is responsible for phenomena such as nonlinear refraction that is referred to the power depending on the nonlinear refractive index (n_2) and the change in the nonlinear phase shift ($\phi_{NL} = n_2 kL\,|E|^2$) since the self-phase modulation (SPM) through circulated inside the NMRR and called the chaos behavior that is Ikeda unstable [10].

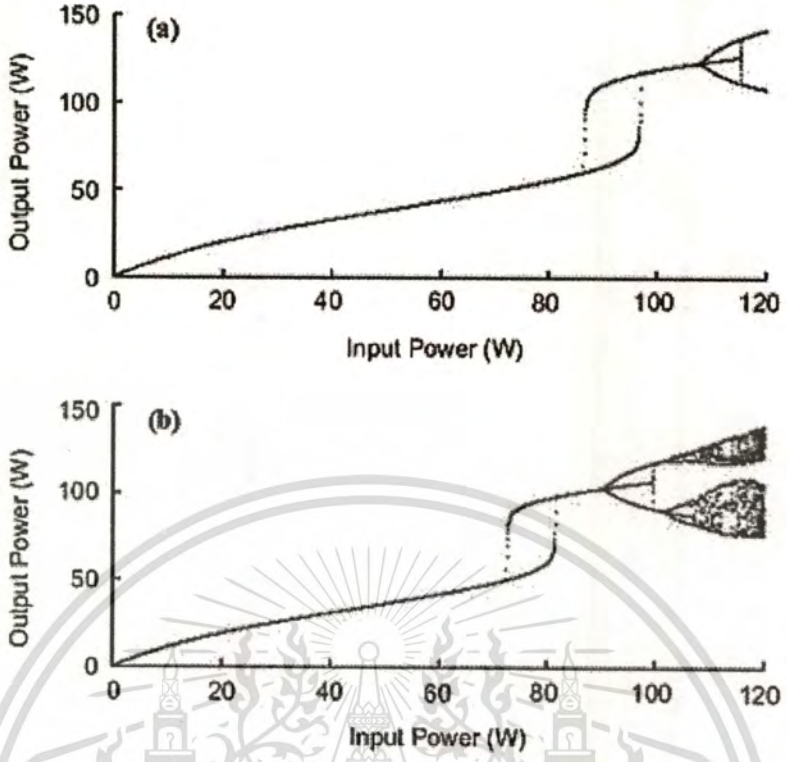

Fig. 3.4 The diagram of optical bistability and bifurcation of the input and output power relation with $\phi_0 = 0$, $K = 0.9$, $L = 80$ m for various nonlinear refractive indices :
(a) $n_2 = 2.2 \times 10^{-20}$ m^2W^{-1} and (b) $n_2 = 2.6 \times 10^{-20}$ m^2W^{-1}

Fig. 3.4(a) shows the nonlinear effects on the bifurcation and bistability diagram in the input and output power relationship for various nonlinear refractive indices (n_2). The region of bistability is obtained in the range of 86.3-97.4 W, Fig. 3.4(b) is ranged in 72.2-81.2 W. The results shows increasing the nonlinear refractive indices can be made the regions of optical bistability occurred in the range of lower input power.

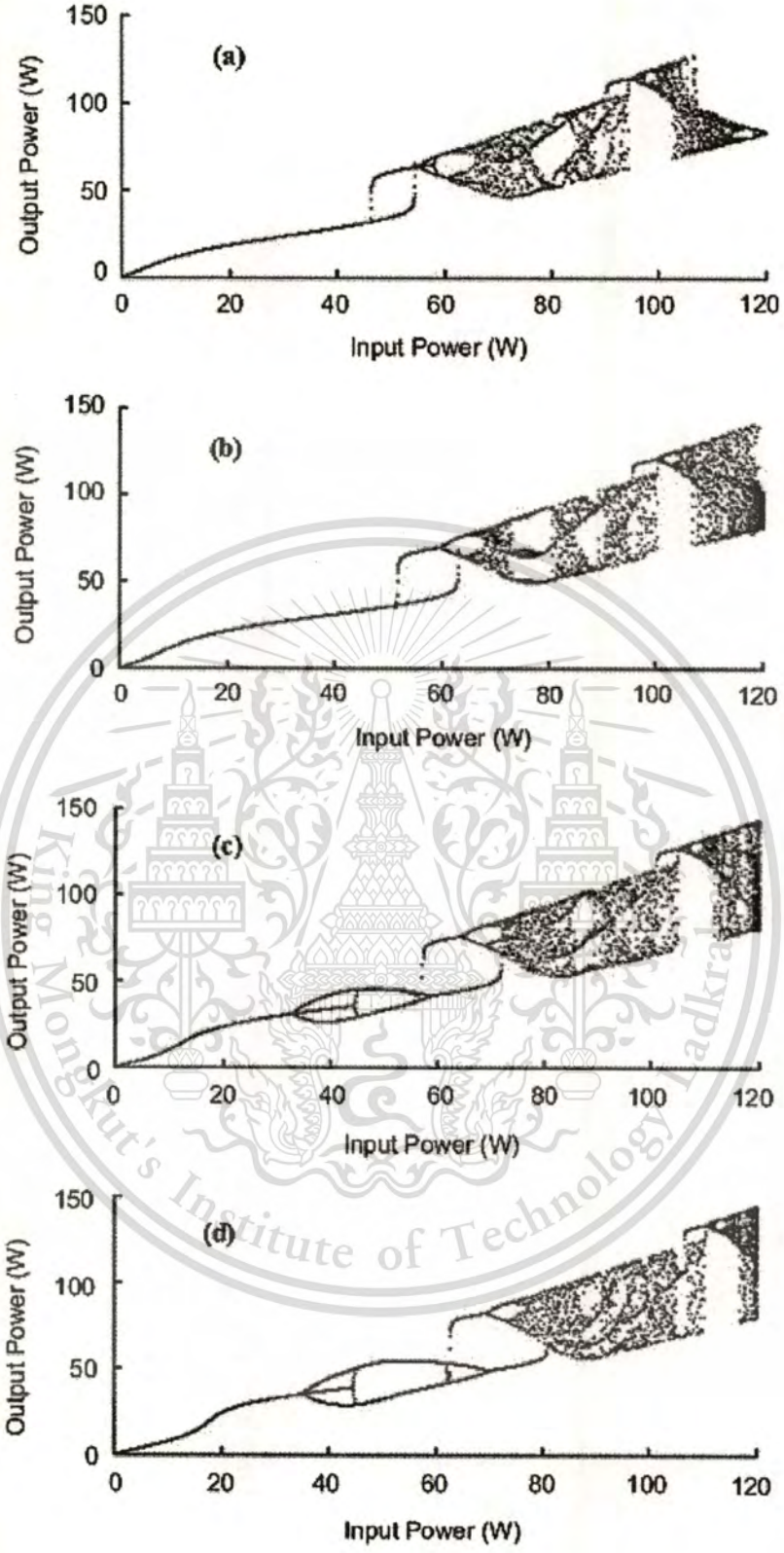

Fig. 3.5 The diagram of optical bistability and bifurcation of the input and output power relation with $n_2 = 3.2 \times 10^{-20}\ m^2W^{-1}$, $K = 0.9$, and $L = 80$ m for various linear phase shifts : (a) $\phi_0 = \pi/4$, (b) $\phi_0 = \pi/2$, (c) $\phi_0 = 3\pi/4$, (d) $\phi_0 = \pi$

Fig. 3.5 is the diagram of optical bistability and bifurcation of the input and output power relation with varying linear phase shift (ϕ_0). Fig. 3.5(a), the optical bistability is found within the range of 46.0-54.6 W and the optical bifurcation occurs at input power 54.6 W, while the optical chaos occurs at input power 60.7 W. Fig. 3.5(b), the optical bistability is found within the range of 51.3-63.3 W and the optical bifurcation occurs at input power 59.5 W, while the optical chaos occurs at input power 64.7 W. Fig. 3.5(c)-(d) the region of optical bistability are the range of 57.0-72.2 and 62.7-81.2 W, respectively.

3.4 Conclusion

This chapter shows the characteristics of FORR and NMRR including the nonlinear phenomena that are the nonlinear refractive index depending on the intensity or the input power, the optical bistability, optical bifurcation and optical chaos. Traveling of light in the NMRR is analyzed numerically by various characterizing of the ring radius, nonlinear refractive index, linear phase shift, and the other important parameters of NMRR.

CHAPTER 4

PULSE POLARIZATION ENTANGLED PHOTON GENERATION

4.1 Entangled Photon Generation

A schematic diagram of polarized photon generated within a micro ring resonator is shown in Fig. 4.1, where the monochromatic light with amplitude E_0 and a random phase ϕ is launched into a micro ring resonator. The input light (E_{in}) can be expressed as

$$E_{in} = E_0 e^{j\phi} \tag{4.1}$$

We assume that the considered nonlinear is Kerr effect, the refractive index is given by

$$n = n_0 + n_2 I = n_0 + \left(\frac{n_2}{A_{eff}}\right) P \tag{4.2}$$

Where n_0 and n_2 are the linear and the nonlinear refractive indices, respectively. I and P are the optical intensity and the optical power, respectively. The effective core area of a micro ring resonator is A_{eff}, which is in the range 0.12-0.50 μm^2. The normalized output can be expressed by

$$\left|\frac{E_{out}}{E_{in}}\right|^2 = (1-\gamma)\left[1 - \frac{(1-(1-\gamma)x^2)\kappa}{(1-x\sqrt{(1-\gamma)(1-\kappa)})^2 + 4x\sqrt{(1-\gamma)(1-\kappa)}\sin^2(\phi/2)}\right] \tag{4.3}$$

Where $x = \exp(-\alpha L/2)$ represents a round-trip losses coefficient, $\phi_L = \phi_0 = kLn_0$ and $\phi_{NL} = kLn_2|E_{in}|^2$ are the linear and the nonlinear phase shifts respectively, $k = 2\pi/\lambda$ is the wave propagation constant in vacuum, κ is the coupling coefficient.

A single light pulse is sliced to be many pulses by the nonlinear behavior, i.e. chaos, which is provided by the increase in entangled photon combination possibility. The parameters of

the system used in the numerical model are fixed to $\lambda_0 = 1.55$ μm, $n_0 = 3.34$, $\alpha = 0.5$ dBmm^{-1}, $\gamma = 0.1$, and R = 10 μm. The coupling coefficient κ ranged from 0.02-0.30. The nonlinear refractive index used is $n_2 = 2.2 \times 10^{-15}$ m^{2}W^{-1} and the data of 20,000 iterations of roundtrips inside the optical micro ring resonator is plotted. We assume that $\phi_{NL} = 0$ for simplicity. However, the change in phase is slightly altered the optical output, which means the dispersion can be neglected when the resonant output is occurred. In general, the input pulse can be a single pulse or pulse trains, where the output pulses after some roundtrips with random polarization are shown in Fig. 4.1. Where the $|H\rangle$ and $|V\rangle$ represent the horizontal and vertical polarization components, respectively.

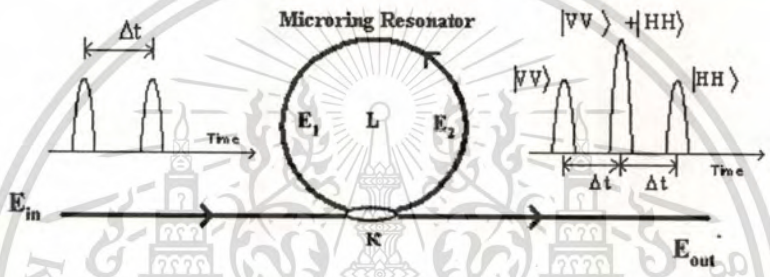

Fig. 4.1 Schematic diagram of a micro ring resonator with a coupling part of a micro ring resonator.

From Fig. 4.1, firstly, a light pulse is launched and chopped to form many pulses by the chaotic behavior within a micro ring resonator. Secondly, we introduce a technique that can be used to create the entangled photon pair. The polarized light can be formed the basic vertical and horizontal polarization states that correspond to the input of short and long pulses. We assume that those horizontally polarized pulses have a temporal separation Δt. When the coupled polarization mode is introduced by the external environment, the following state is created by

$$|\psi\rangle = |1,H\rangle_s|1,H\rangle_i + |2,H\rangle_s|2,H\rangle_i \tag{4.4}$$

In the expression $|n,H\rangle$, n is the number of time slots (1 or 2), where the $|H\rangle$ and $|V\rangle$ represent the state of polarization in horizontal and vertical components, respectively. The subscript identifies whether the state is in the signal (s) or the idler (i). In Eq. (4.4), for simplicity

we have omitted an amplitude term that is common subsequent equation in this thesis. This two photon state with $|H\rangle$ polarization shown by Eq. (4.4) is input into the orthogonal polarization-delay circuit that is shown schematically in Fig. 4.1. The delay circuit consists of a coupler and the difference between the round-trip times of the micro ring resonator, which is equal Δt. The light signal within a micro ring resonator is coupled and converted into $|V\rangle$ at the delay circuit output, then Eq. (4.4) is converted into the polarized state by the delay circuit as

$$\begin{aligned}|\psi\rangle &= \left(|1,H\rangle_s + \exp(i\phi_s)|2,V\rangle_s\right)\times\left(|1,H\rangle i + \exp(i\phi_i)|2,V\rangle_i\right)+ \\ &\quad \left(|2,H\rangle_s + \exp(i\phi_s)|3,V\rangle_s\right)\times\left(|2,H\rangle_i + \exp(i\phi_i)|2,V\rangle_i\right) \\ &= \left(|1,H\rangle_s|1,H\rangle_i + \exp(i\phi_i)|1,H\rangle_s|1,V\rangle_i\right)+\left(\exp(i\phi_s)|2,V\rangle_s|1,H\rangle_i\right)+ \\ &\quad \left(\exp(i\phi_i+i\phi_s)|2,V\rangle_s|2,V\rangle_i\right)+\left(|2,H\rangle_s|2,H\rangle_i\right)+\left(\exp(i\phi_i)|2,H\rangle_s|3,V\rangle_i\right)+ \\ &\quad \left(\exp(i\phi_s)|3,V\rangle_s|2,H\rangle_i\right)+\left(\exp(i\phi_i+i\phi_s)|3,V\rangle_s|3,V\rangle_i\right)\end{aligned} \tag{4.5}$$

By the coincidence counts in the second time slot, we can extract the fourth and fifth terms, As a result, we can obtain the following polarization entangled state as

$$|\psi\rangle = |2,H\rangle_s|2,H\rangle_i + \exp(i\phi_s+i\phi_i)|2,V\rangle_s|2,V\rangle_i \tag{4.6}$$

We assume that the response time of the Kerr effect is much less than the cavity round-trip time. Because of the Kerr nonlinearity of the optical device, strong pulses acquire an intensity dependent phase shift during propagation. The interference of light pulses at the coupler introduces the superposition of light, which is entangled. Due to the polarization, states of light pulses are changed and converted while circulating in the delay circuit where the polarization entangled photon pairs can be generated. The entangled photons of the nonlinear ring resonator are separated to be the signal and the idler photons. A polarization angle adjustment device is used to investigate the orientation and the optical output intensity where the compensation, i.e. the measurement, is performed.

Generally, there are two pairs of possible polarization entangled photons, which are represented by the four polarization orientation angles as [0°,90°] and [135°,180°]. They can be formed by using a quarter wave plate after the polarization rotation device and the polarizing beam splitter. However, in practice, a continuously variable entangled photon can be generated,

which introduces the possibility that a random entangled photon pair can be formed from the photon visibility. To generate the polarized photons, a rotatable polarizer in included in the system after the ring device as shown in Fig. 4.2. The output polarized state is controlled by a rotatable polarizer, where the input azimuth angle is changed to obtain the required state. The randomly polarized light is formed the specific angle by controlling the rotatable polarizer and polarization beam splitter (PBS). The two orthogonal polarized modes ($|H\rangle$ and $|V\rangle$) are performed and detected by the two detectors. By rotating the azimuth angles from 0-180°, the polarization entangled photon visibility is plotted and seen.

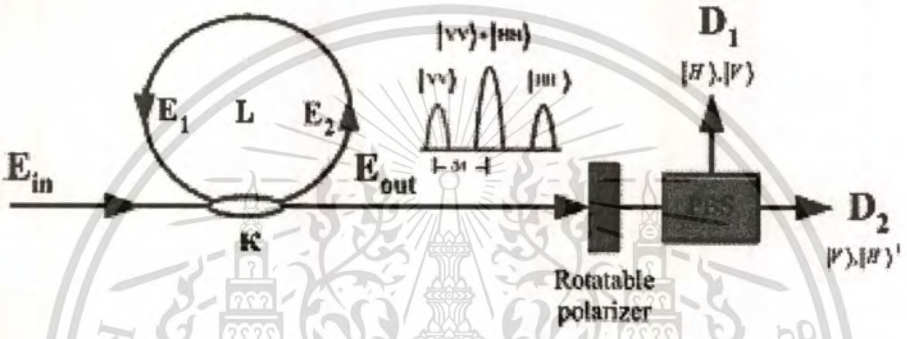

Fig. 4.2 A schematic of the entangled photon generation and detection system ; PBS : Polarization Beam Splitter, D : Detectors.

We assume that polarization rotation of light traveling through the optical device is represented by the rotation matrix (M)

$$M(\theta) = R(\theta)MR(-\theta) \tag{4.7}$$

Where

$$R(\theta) = \begin{bmatrix} \cos\theta & -\sin\theta \\ \sin\theta & \cos\theta \end{bmatrix} \text{ Counterclockwise rotation by } \theta \tag{4.8}$$

And

$$R(-\theta) = \begin{bmatrix} \cos\theta & \sin\theta \\ -\sin\theta & \cos\theta \end{bmatrix} \text{ Clockwise rotation by } \theta \tag{4.9}$$

where θ is the polarization azimuth angle.

The optical intensity of polarization entangled photon that is generated by NMRR, can be given by the adjusting of the polarization angle of the rotatable polarizer from 0° to 180° before launching into the polarization beam splitter (PBS). Then the polarization photons can be detected by using the photodetector such as avalanche photodetector (APD). The relation between optical intensity and each polarization photon with phase difference are plotted in Fig. 4.3.

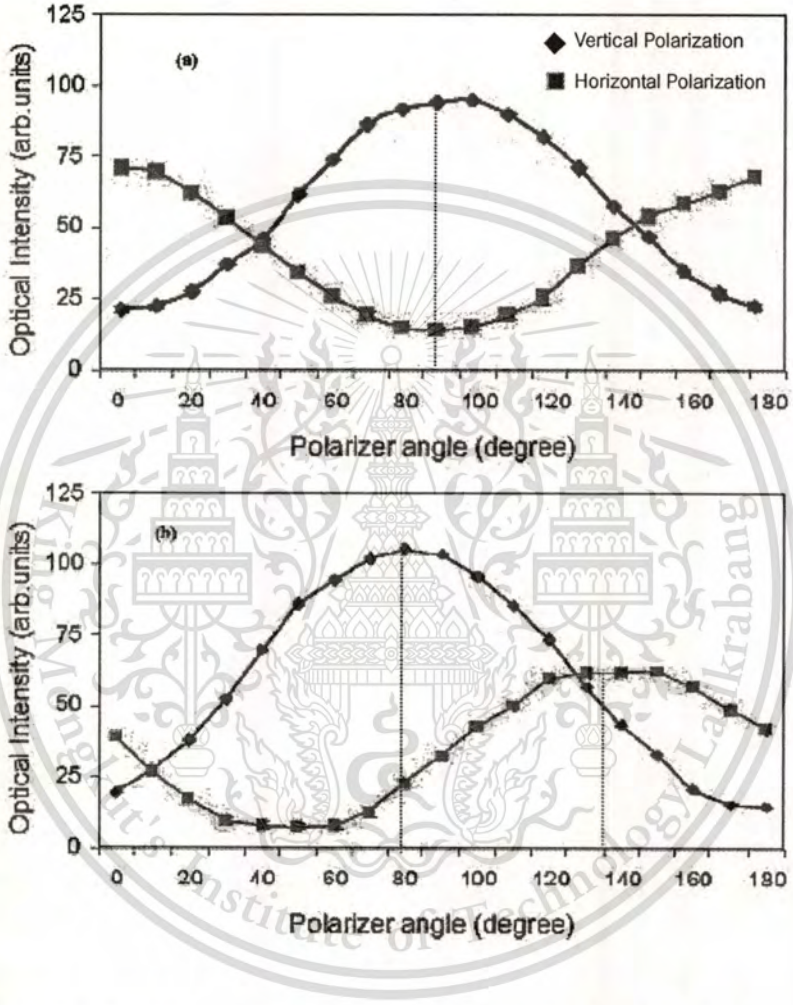

Fig. 4.3 The graphs of optical intensity of polarization entangled photon that is generated from NMRR with the phase difference, where (a) $\phi = 0^{\circ}$, (b) $\phi = 55^{\circ}$

The investigation of the output light characteristics within the optical micro ring resonator is described as following details. A Gaussian input pulse with peak power at 4.25 mW is input into the resonator via the input port. The parameters of a system are $\lambda_0 = 1.55$ μm, $n_0 = 3.34$, $\alpha = 0.5$ dBmm^{-1}, $\gamma = 0.1$, and R = 10 μm. The coupling coefficient κ ranged from 0.02-0.30 for the polarization output intensity and from 0.3-0.7 for the chaotic signal output intensity.

The nonlinear refractive index is $n_2 = 2.2 \times 10^{-15}$ m^2W^{-1} and the data of 20,000 iterations of roundtrips inside the optical micro ring resonator is plotted. To generate the optimum possibility of four-wave mixing of polarized light, where the nonlinear effect can be well performed, therefore, the chaotic oscillation is introduced into the system. The completed chaotic signals occur within the roundtrips as shown in Fig. 4.4.

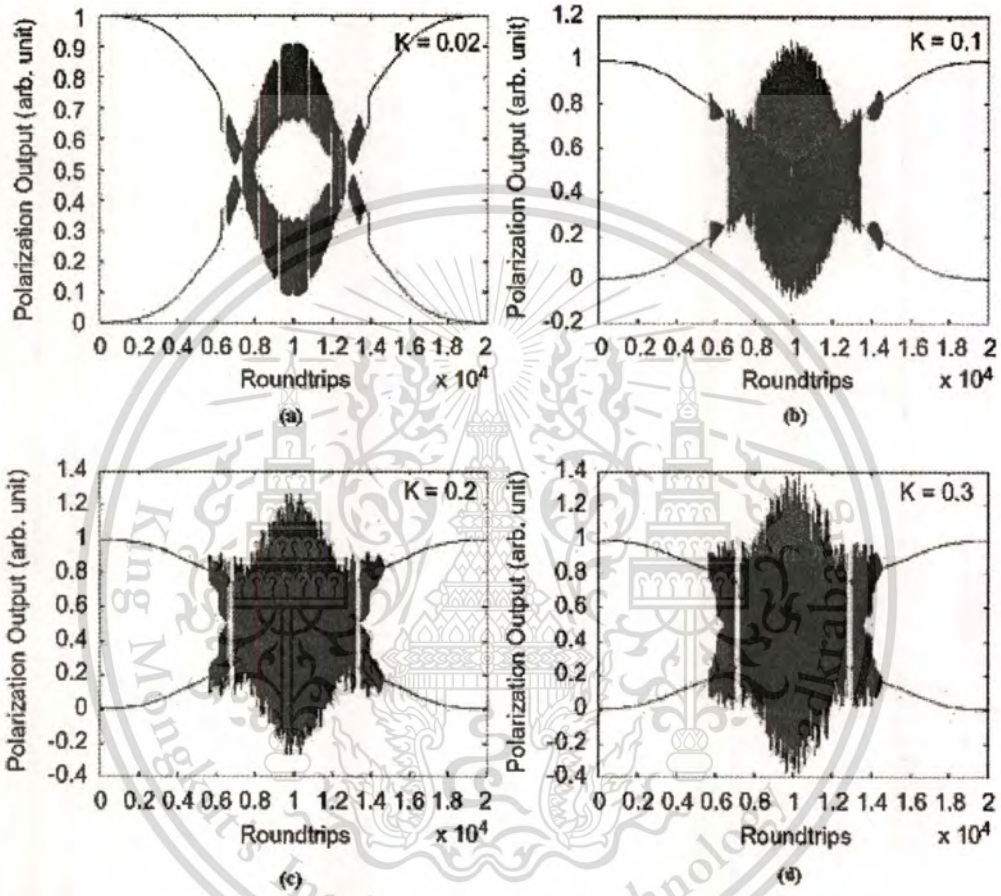

Fig. 4.4 The polarization output of the chaotic signals with different coupling coefficients, where green (top) and blue (bottom) represent horizontal and vertical polarized lights, respectively. (a) $\kappa = 0.02$, (b) $\kappa = 0$, (c) $\kappa = 0.2$ and (d) $\kappa = 0.3$

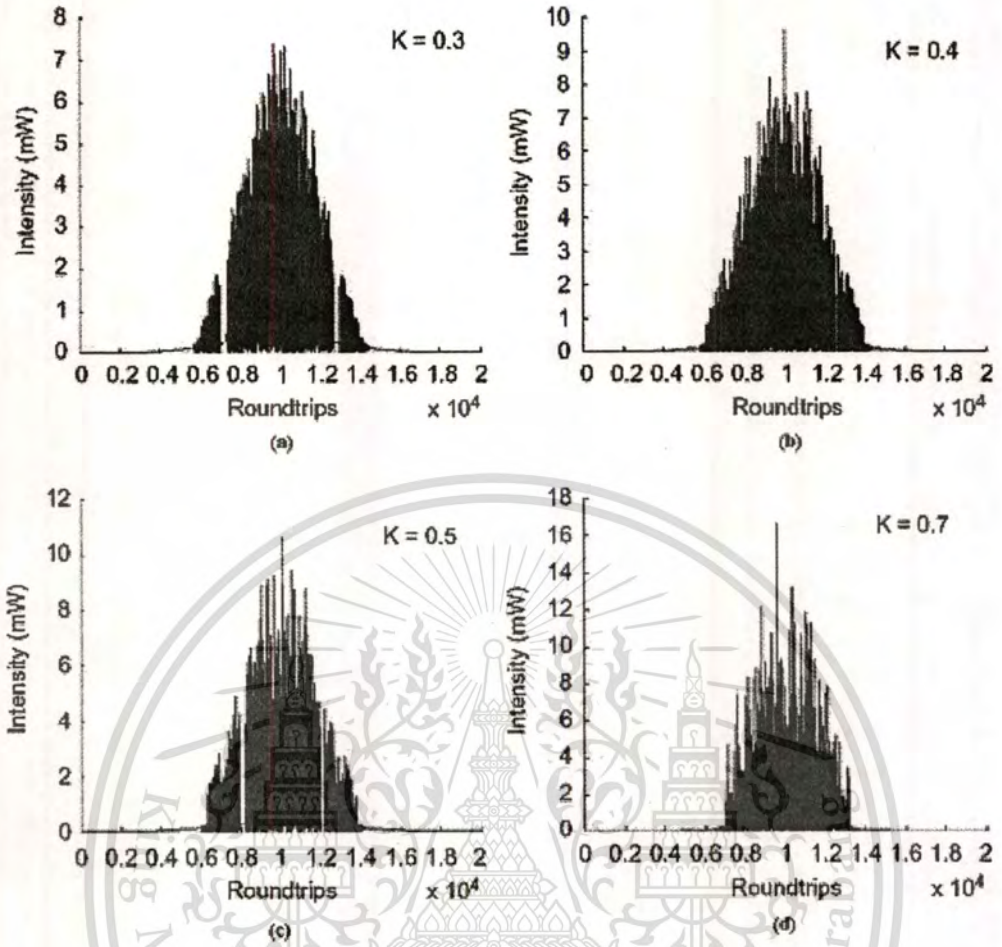

Fig. 4.5 The output of the chaotic signals, where various the coupling coefficients : (a) $\kappa = 0.3$, (b) $\kappa = 0.4$, (c) $\kappa = 0.5$ and (d) $\kappa = 0.7$.

In principle, the quantum chaotic behaviors can be described by using the Jones matrix representation. When the chaotic signal is generated then passing through the rotatable polarizer and polarization beam splitter. The required azimuth angle is adjusted to obtain the specific orientation angle via the rotatable polarizer. The random entangled photon pair is split via a PBS and detected by the two detectors. In general, the entangled photon pairs may be formed by two different forms of the orientation angles (0°, 90°) or (135°, 180°), which is represented by light travelling into the optical components as described earlier.

4.2 Conclusion

This chapter has demonstrated the polarization entangled photon generation by using a nonlinear effects inducing within a micro ring resonator. The results of demonstration shows two pairs of the orthogonal polarized modes can be formed and detected by using the system in Fig. 4.1 and 4.2. Beside that, the chapter describes the polarization state of entangled photon that propagated along the nonlinear micro ring resonator and used a rotatable polarizer and a polarization beam splitter to detect it.

CHAPTER 5

BIREFRINGENCE BASED SENSING APPLICATIONS

5.1 Birefringence Based Sensor

A simple schematic of a nonlinear micro ring resonator (NMRR) for birefringence based sensing applications is shown in Fig. 5.1.

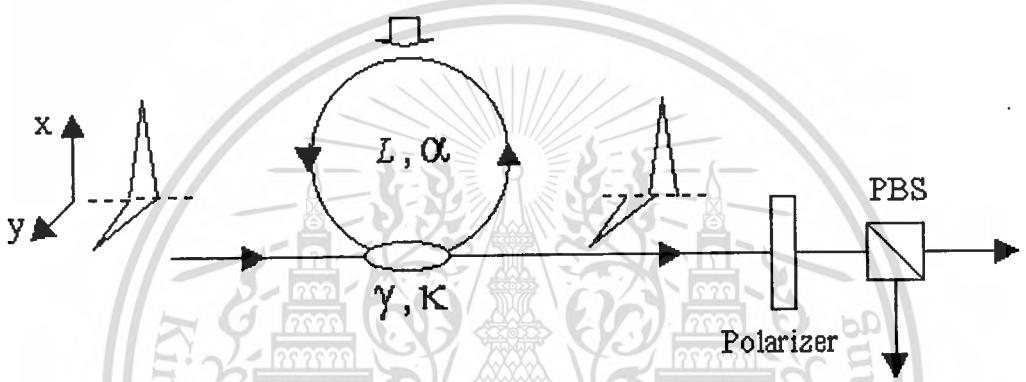

Fig. 5.1 A schematic of a nonlinear micro ring resonator for birefringence based sensor ; PBS : Polarization beam splitter.

The system consisted of a nonlinear micro ring resonator based on birefringence. When the polarized light is propagated into a nonlinear micro ring resonator that is stress-induced material birefringences, thus the polarization mode dispersion (PMD) is occurred. PMD is a modal dispersion when two orthogonal polarizations of light are propageted into an ideal optical fiber, which normally propagated at the same speed. Because of the stress-induced material birefringences, causing the two orthogonal polarizations propagated with different speeds. Birefringence effect can be formalised by assigning two different refractive indices correspond to the different speeds. The birefringence magnitude is defined as the difference between the refractive index in two axises, as $\Delta n = n_x - n_y$ where n_x and n_y are the refractive index of the polarized light along the fast and slow axis respectively. The PMD compensation can be used many process such as using a polarization controller to compensate for PMD in optical fiber,

using a polarization maintaining fiber (PM fiber), and projecting the output light into a polarization beam splitter then found the phase difference. The relationship between phase difference and birefringence can be given by

$$\Delta\phi = \frac{2\pi(n_x - n_y)L}{\lambda} \tag{5.1}$$

From Fig. 5.1, the parameters of the system are λ = 1.55 μm, n = 1.45, κ = 0.1, γ = 0.15, α = 0.02 dB/km, R = 100 μm. First, no birefringence $\Delta n = n_x - n_y = 0$ or no stress-induced, the polarized lights from a NMRR is separated into vertical polarized light and horizontal polarized light by using PBS. The two orthogonal polarized lights have a same phase (phase difference equal zero). When a NMRR is induced by external stress, the birefringence occurs. The two orthogonal polarized light have the different phase. The phase difference can be found by using the rotatable polarizer adjusting of the polarization angle from 0° to 360° (or 0 - 2π). From Eq. 3.8 and Eq. 5.1, the relationship between the normalized output intensity and the phase shift is shown in Fig. 5.2. The numerical result obtained show that the phase shift is 0.35 radian or 20.05 degree.

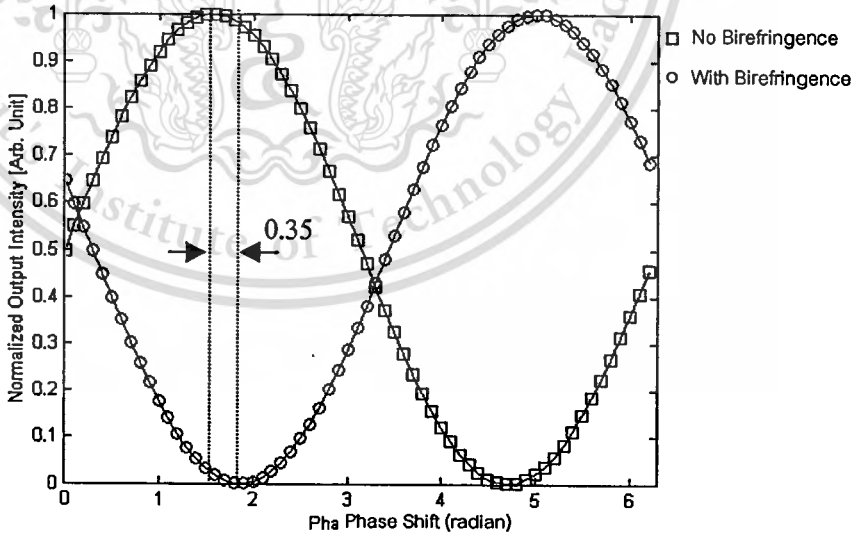

Fig. 5.2 The two orthogonal polarizations propagated with phase difference 0.35 radian.

From a system, it can be used to the sensing applications based using birefringence concepts such as the micro gyroscope sensor based a nonlinear micro ring resonator. The benefit of a micro ring resonator that can be reduced the device scale in the micron regime to measure more possible application.

5.2 Walk-off Compensation

When polarized light propagates in fiber optic, the change in birefringence is introduced. This means the changed in phase of the entangled photon pair is occurred. Where the transversal walk-off produces a shift between the ordinary and extraordinary, while the longitudinal walk-off introduces a time delay between horizontally and vertically polarized photons. The amount of the walk-off depends on the location where the photon-pairs are created within the fiber. This position is completely random due to the coherent nature of light in fiber optic. To compensate the longitudinal timing-walk off effect, a polarization controller is recommended to ensure that the polarization rotation is the same on both photons from the entangled pair. Additionally the compensator fiber is used to change the relative phase (ϕ) of the states of the polarized light. Because of the change in birefringence, the tilting of the compensator allows to apply a phase shift to the entangled states of the two entangled photons, which is given by Eq. (5.2).

$$|\psi\rangle_{12} = \frac{1}{\sqrt{2}}\left(|H\rangle_1|V\rangle_2 + e^{i\phi}|V\rangle_1|H\rangle_2\right) \tag{5.2}$$

In applications, the walk-off entangled state parameters involving in the measurement are related to the changes in the applied physical parameters such as force, stress, strain, heat, and pressure etc and the fiber optic properties. However, the interested parameters in this proposed systems are concerned the fiber optic birefringence parameters, which can be given by

$$\Delta\phi = \frac{2\pi(n_x - n_y)L_w}{\lambda} \tag{5.3}$$

Where $\Delta n = n_x - n_y$ is the fiber optic birefringence, L_w is the entangled states walk-off length, and λ is the light source wavelength.

5.3 Conclusion

This chapter shows a simple model of a nonlinear micro ring resonator (NMRR) for birefringence based sensing applications. The system consists of a NMRR inducing by external stress. The results is the polarization mode dispersion (PMD) causing the birefringence. The birefringence magnitude is given by the difference between the refractive index in two axises, as $\Delta n = n_x - n_y$. The birefringence compensation can be used the many process such as using a polarization controller to compensate for PMD in optical fiber, using a polarization maintaining fiber (PM fiber), projecting the output light into a polarization beam splitter then found the phase difference, and the walk-off compensation.

CHAPTER 6

CONCLUSION

This thesis proposes a concept of pulse polarization entangled photon that is generated by using the nonlinear micro ring resonator. The application of this system is the birefringence based sensor using the entangled photon walk-off compensation. First, to study the nonlinear effects in micro ring resonator such as optical Kerr effect, nonlinear refraction, four-wave mixing, and nonlinear birefringence. Then, to assign the appropriate parameters of the micro ring resonator for using generated polarization entangled photon. The possible entangled photon pairs can be detected by using the external polarizer, polarization beam splitter, and photodetector (APD). The designed system can be used to the birefringence sensing by finding the relation between the applied physical parameters such as temperature, pressure, etc., and the changed birefringence. Results obtained have shown that the possible system can be generated the pulse polarization entangled photon by using the nonlinear micro ring resonator and using for birefringence based sensing application.

First, we describe the light propagation equation in optical fibers by using Maxwell's equation and describes the nonlinear effects that are occurred in optical fibers, such as the third-order susceptibility, nonlinear refractive index and nonlinear Kerr effects. Then, shows the nonlinear refraction depending on the light intensity and referred to SPM and XPM. Third, describes the optical Kerr effect occurred from the intensity of electric field. After that, explains the FWM creating an output light at frequency ω_3 and ω_4 from input light at frequency ω_1 and ω_2 by using nonlinear susceptibility $\chi^{(3)}$. Finally, describes the nonlinear birefringence that is occurred from the unequal of the effective refractive indices, n_x and n_y along the principal axes of the optical fibers. This is caused the slow and fast axes of the speed of light that travels inside the fiber. Beside that, if a sufficiently intense light are launched into optical fiber, the nonlinear birefringence can be induced where amplitude is intensity dependent.

Second, we show the important characteristics of fiber optic ring resonator (FORR) and nonlinear micro ring resonator (NMRR) including the nonlinear phenomena such as the nonlinear refractive index depending on the intensity or the input power, the optical bistability, optical bifurcation and optical chaos. Traveling of light in the NMRR is analyzed numerically by various

characterizing of the ring radius, nonlinear refractive index, linear phase shift, and the other important parameters of NMRR.

Third, we have demonstrated the polarization entangled photon generation by using a nonlinear effects inducing within a NMRR. The results of demonstration shows two pairs of the orthogonal polarized modes can be formed and detected by using the system in Fig. 4.1 and 4.2. Beside that, the chapter describes the polarization state of entangled photon that propagated along the NMRR and used a rotatable polarizer and a polarization beam splitter to detect it.

Finally, we show a simple model of a NMRR for birefringence based sensing applications. The system consists of a NMRR inducing by external stress. The nonlinear birefringence is occurred. The birefringence magnitude is given by the difference between the refractive index in two axises, as $\Delta n = n_x - n_y$. The birefringence compensation can be used the many process such as using a polarization controller to compensate for PMD in optical fiber, using a polarization maintaining fiber (PM fiber), projecting the output light into a polarization beam splitter then found the phase difference, and timing walk-off compensation.

REFERENCES

[1] P.P. Yupapin, "Fiber optic sensing appliction using the entangled states walk-off compensations", **International Journal of Light and Electron Optics**, 2007.

[2] R. Grover, P.P. Absil, V. Van, J. V. Hryniewicz, B. E. Little, O. King, L. C. Calhoun, F. G. Johnson, and P.-T. Ho, "Vertically coupled GaInAsP–InP microring resonators", **Opt. Lett.**, 26(2001) 506.

[3] P.P. Yupapin and W. Suwancharoen, "Chaotic signal generation and cancellation using a micro ring resonator incorporating an optical add/drop multiplexer", **Optic Commun.**, 280(2007) 343.

[4] P.P. Yupapin, W. Khunnam and S. Suchat, "The entangled photons generation system using weak light in fiber optic and timing walk-off compensation", **International Journal of Quantum Information**, 5(2007) 805.

[5] C. Sripakdee, K. Sarpat, W. Suwancharoen and P.P. Yupapin, "Entangled photon generation in a nonlinear micro ring resonator for quantum key distribution use", **Proc. in SmarMat-08 & IWOFM-2**, Chiang Mai, 2008.

[6] C. Fietz and G. Shvets, "Nonlinear polarization conversion using micro ring resonstors", **Opt. Lett.**, 32(2007) 1683.

[7] H. Takesue, K. Inoue, O. Tadanaga, Y. Nishida and M. Asobe, "Generation of Pulsed Polarization-Entangled Photon Pairs in a 1.55-μm Band with a Periodically Poled Lithium Niobate Waveguide and an Orthogonal Polarization Delay Circuit", **Opt. Lett.**, 30(2005) 293.

[8] P.P. Yupapin and W. Khunnam, "An Investigation of the Entangled Photon Walk-off Compensation Generated by a Fiber Ring Resonator", **International Journal of Light and Electron Optics**, 2008.

[9] C. Silberhorn C., P. Lam, O. Weib, F. Konig, N. Korolkova, G. Leuchs, "Generation of continous variable Einstein-Podolsky-Rosen entanglement via the Kerr nonlinearity in an optical fiber", **Phys. Rev. Lett.**, 86(2001) 4267-4270.

[10] K. Ikeda, H. Daido, O. Akimoto, "Optical turbulence : chaotic behavior of transmitted light from a ring-cavity", **Phys. Rev. Lett.**, 45(1980) 709-712.

REFERENCES (Cont.)

[11] K. Ogusu, H. Shigekuni, Yokota, "Dynamic transmission properties of a nonlinear fiber ring resonator", **Opt. Lett.**, 20(1995) 2288-2290.

[12] J.H. Marburger, F.S. Felber, "Theory of a lossless nonlinear Fabry-Perot interferometer", **Phys. Rev. A**, 17(1978) 335-342.

[13] T. Bischofberger, Y.R. Shen, "Theoretical and experiment study of the dynamic behavior of a nonlinear Fabry-Perot interferometer", **Phys. Rev. A**, 19(1979) 1169-1176.

[14] H. Nakatsuka, S. Asaka, H. Itoh, K. Ikeda, and M. Matusuoka, "Observation of bifurcation to chaos in an all-optical bistable system", **Phys. Rev. Lett.**, 50(1983) 109-112.

APPENDIX

LIST OF PUBLICATIONS

[1] N. Pornsuwancharoen, P. Phiphithirankarn, P.P. Yupapin, and J. Ali, **Pulse Polarization Entangled Photon Generated by Chaotic Signals in a Nonlinear Micro Ring Resonator for Birefringence Based Sensing Applications**, ELSEVIER : Optics and Laser Technology, Vol. 41, 2009, pp. 788-793. (DOI:10.1016/j.optlastec.2008.12.009)

[2] P. Chunpang, P. Phiphithirankarn, and P.P. Yupapin, **An Investigation of Quantum Chaotic Signals Generation using a Fiber Ring Resonator and an Add/Drop Multiplexer**, ELSEVIER : Optik - International Journal for Light and Electron Optics, 2009. (DOI:10.1016/j.ijleo.2008.09.023)

[3] P. Phiphithirankarn, P. Yabosdee, and P.P. Yupapin, **Nonlinear Effects in Fiber Grating to Nano Scale Measurement Resolution**, World Scientific : Journal of Nonlinear Optical Physics & Materials (JNOPM), Special Issue Volume, November, 2008.

[4] P.P. Yupapin, P. Yabosdee, and P. Phiphithirankarn, **Entangled photon generation in a nonlinear micro ring resonator for birefringence based sensing application**, ELSEVIER : Optik – International Journal for Light and Electron Optics, 2008. (DOI:10.1016/j.ijleo.2008.07.024)

[5] P. Yabosdee, P. Phiphithirankarn, and P.P. Yupapin, **A new concept of nano strain monitoring using μ-strain perturbation**, ELSEVIER : Optik - International Journal for Light and Electron Optics, 2008. (DOI:10.1016/j.ijleo.2008.07.028)

[6] P. Phiphithirankarn, P. Yabosdee, W. Suwancharoen, and P.P. Yupapin, **Novel Design of a Micro Gyroscope Based Birefringence Measurement for Sensor Applications**, Scientific : Advanced Materials Research, Vol. 55-57, 2008, pp. 521-524.

[7] P. Phiphithirankarn, P. Yabosadee, and P.P. Yupapin, **Nonlinear Effects in Fiber Grating to Nano-Scale Measurement Resolution**, Proceeding SPIE, Vol. 6793, 67930S, 2007. (DOI:10.1117/12.799533)

[8] P.P. Yupapin, P. Phiphithirankarn, and S. Suchat, **A Quantum CODEC Design via an Optical Add/Drop Multiplexer in a Fiber Optic Network**, Far East Journal of Electronics and Communications, Vol.1(3), 2007, pp. 259-267.

Optics & Laser Technology 41 (2009) 788–793

Contents lists available at ScienceDirect

Optics & Laser Technology

journal homepage: www.elsevier.com/locate/optlastec

Pulse polarization entangled-photon generated by chaotic signals in a nonlinear micro-ring resonator for birefringence-based sensing applications

N. Pornsuwancharoen [a], P. Phiphithirankarn [b], P.P. Yupapin [b,*], J. Ali [c]

[a] Department of Electrical Engineering, Faculty of Industry and Technology, Rajamangala University of Technology Isan, Sakonnakon 47160, Thailand
[b] Advanced Research Center for Photonics, Faculty of Science, King Mongkut's Institute of Technology Ladkrabang, Chalongkrung Road, Ladkrabang, Bangkok 10520, Thailand
[c] Institute of Advanced Photonics Sciences, Science Faculty, Universiti Teknologi Malaysia, 81310 Skudai, Johor Bahru, Malaysia

ARTICLE INFO

Article history:
Received 10 April 2008
Received in revised form
3 December 2008
Accepted 5 December 2008
Available online 3 February 2009

Keywords:
Birefringence sensor
Polarized entangled photon
Nonlinear micro-ring resonator

ABSTRACT

We propose a new concept of birefringence-based sensing using entangled-photon timing-walk-off compensation. Four-wave mixing within a micro-ring resonator is employed, which is introduced by the nonlinear Kerr effect. The two possible entangled photon pairs are randomly formed by using an external polarization control unit. Results obtained have shown that the entangled-photon walk-off state within the ring device can be compensated. This means that the changes in walk-off-state parameters can be measured in response to changes in the applied physical parameters. The experimentally determined relationship between temperature and the entangled-photon walk-off parameter is seen to be in good agreement with the theoretical predictions. The potential of using the proposed system for the development of birefringence-based sensing systems is discussed.

1. Introduction

Yupapin [1] has reported on the concept of an ultrahigh measurement resolution method using polarized photons in a fiber optic ring resonator. He has concluded that the shift in optimum entangled photon visibility can be compensated by appropriate walk-off length, where the measurement resolution is increased by the order of the change in material birefringence. Alternatively, optical micro-ring resonators have been widely investigated both theoretically and experimentally. It has been found that the device scale is dramatically decreased. Devices of dimensions of few microns have been fabricated and are available [2]. One of the promising application aspects is that the small device in which the secure message can be stored within the device, can be fabricated. For instance, the techniques such as chaos [3,4], quantum entanglement [5,6] and chaotic quantum [7] have shown potential applications. Recently, Fietz and Shvets [6] reported that polarized entangled photons can be generated by using a micro-ring device [8]. Suchat et al. [9] have demonstrated entangled photon recovery, i.e. regeneration using a fiber optic ring resonator incorporating an EDFA, which is useful for long-distance links. However, polarization dispersion causes the entangled photon to encounter a problem called timing walk-off, which becomes an issue in the recovery process.

In this paper, we design a micro-ring device to form the polarized entangled photons for sensing applications. The entangled photon generation and their behavior within the proposed device are analyzed and discussed. Results obtained show that there is a good potential for the use of such a device for birefringence-based sensing applications, where the measurement of physical parameters such as temperature, pressure and moisture is plausible.

2. Operating principle

A schematic diagram of a ring device is shown in Fig. 1, where light from a monochromatic light source is launched into a ring resonator with a constant light field amplitude (E_0) and with a random phase modulation (ϕ_0) as a function of time (t), which results in temporal coherence degradation. Hence, input light field (E_{in}) can be expressed as

$$E_{in}(t) = E_0 \exp^{j\phi_0(t)} \quad (1)$$

We assume that the nonlinearity of the optical ring resonator is of the Kerr type, i.e., the refractive index is given by

$$n = n_0 + n_2 I = n_0 + \left(\frac{n_2}{A_{eff}}\right) P \quad (2)$$

where n_0 and n_2 are the linear and the nonlinear refractive indices, respectively. I and P are the optical intensity and the optical field power, respectively. The effective mode core area of the device is A_{eff}, which is in the range 0.12–0.50 μm².

* Corresponding author. Tel.: +662 9647882; fax: +662 3264354.
E-mail address: kypreech@kmitl.ac.th (P.P. Yupapin).

0030-3992/$ - see front matter © 2008 Elsevier Ltd. All rights reserved.
doi:10.1016/j.optlastec.2008.12.009

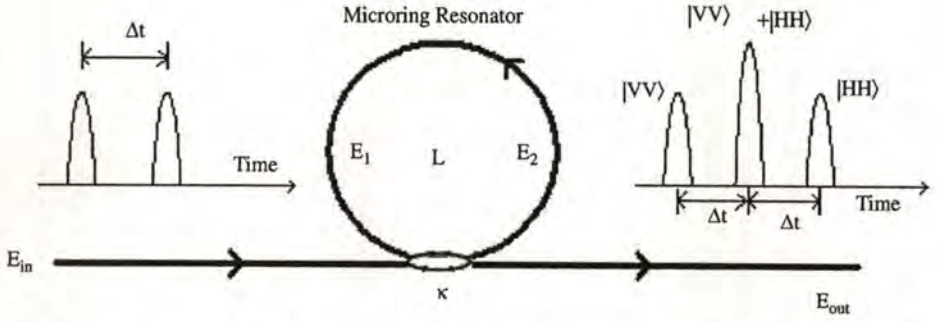

Fig. 1. A schematic diagram of polarized photon generated within a micro-ring resonator and the polarized entangled photon components.

Thus, the normalized output light of the system shown in Fig. 2 can be expressed by [4]

$$\left|\frac{E_{out}(t)}{E_{in}(t)}\right|^2 = (1-\gamma)\left[1-\frac{(1-(1-\gamma)x^2)\kappa}{(1-x\sqrt{1-\gamma}\sqrt{1-\kappa})^2+4x\sqrt{1-\gamma}\sqrt{1-\kappa}\sin^2(\phi/2)}\right] \quad (3)$$

where $x=\exp(-\alpha L/2)$ represents the one round-trip losses coefficient, $\phi_0 = kLn_0$ and $\phi_{NL} = kLn_2|E_m|^2$ are the linear and the nonlinear phase shifts respectively, $k=2\pi/\lambda$ is the wave propagation constant in vacuum and the coupling coefficient is κ. A close examination of Eq. (3) indicates that a ring resonator is similar to a Fabry–Perot cavity, which has an input and output mirror with a field reflectivity, $1-\kappa$, and a fully reflecting mirror.

The key point of this work is that a single light pulse is sliced to be many pulses by the nonlinear behavior, i.e. chaos, which is provided by the increase in entangled photon combination possibility. The parameters of the system used in the theoretical model are fixed to $\lambda_0 = 1.55\,\mu m$, $n_0 = 3.34$, $A_{eff} = 50\,\mu m^2$, where the waveguide (ring resonator) loss $\alpha = 0.5\,dB\,mm^{-1}$. The bending loss of the waveguide used (for InGaAsP/InP) was confirmed by Ref. [4], where the propagation loss used is as low as $1.3\pm.02\,dB\,mm^{-1}$ at $1.55\,\mu m$. The fractional coupler intensity loss is $\gamma = 0.1$ and $R_1 = 10\,\mu m$. The coupling coefficient (κ) ranged from 0.02 to 0.30. The nonlinear refractive index used $n_2 = 2.2\times10^{-15}\,m^2\,W^{-1}$, and the data of 20,000 iterations (a resonant peak is obtained) of roundtrips inside the optical micro-ring is plotted. We assume that $\phi_{NL}=0$ for simplicity. However, the change in nonlinear phase shift slightly alters the optical output, which means that dispersion can be neglected when resonant output is obtained. In general, the input pulse can consist of a single pulse or of pulse trains, where the output pulses after some roundtrips with random polarization are in the form shown in Fig. 1. $|H\rangle$ and $|V\rangle$ represent the horizontal and the vertical polarization components, respectively.

To begin this concept, firstly, a light pulse is input and chopped to form many pulses by the chaotic behavior within the micro-ring resonator. Secondly, we introduce a technique that can be used to create the entangled photon pair (qubits) as shown in Fig. 1 [10]. Polarized light can be formed from the basic vertical and horizontal polarization states that correspond to the input of short and long pulses. We assume that those horizontally polarized pulses have a temporal separation Δt. The coherence time of the consecutive pulses is larger than Δt. When the coupled polarization mode is introduced by the external environment, the following state is created by Eq. (4):

$$|\Phi\rangle_p = |1,H\rangle_s|1,H\rangle_i + |2,H\rangle_s|2,H\rangle_i \quad (4)$$

In the expression $|k,H\rangle$, k is the number of time slots (1 or 2), where $|H\rangle$ and $|V\rangle$ denote the state of polarization in horizontal and vertical components, respectively, and the subscript identifies whether the state is in the signal (s) or the idler (i) state. In Eq. (4), for simplicity we have omitted an amplitude term that is common to all product states. We employ the same simplification in subsequent equations in this paper. This two-photon state with $|H\rangle$ polarization shown by Eq. (4) is input into the orthogonal polarization-delay circuit shown schematically in Fig. 1. The delay circuit consists of a coupler and the difference between the round-trip times of the micro ring resonator, which is equal to Δt. The light signal within a micro-ring resonator is coupled and converted into $|V\rangle$ at the delay circuit output. That is the delay circuits can be converted to the form

$$|k,H\rangle \text{ to } r|k,H\rangle + t_2\exp(i\phi)|k+1,V\rangle + rt_2\exp(i_2\phi)|k+2,H\rangle + r_2t_2\exp(i_3\phi)|k+3,V\rangle$$

where t and r are the amplitude transmittances of the cross and bar ports in the coupler. Then Eq. (4) is converted into the polarized state by the delay circuit as

$$\begin{aligned}|\Phi\rangle &= [|1,H\rangle_s + \exp(i\phi_s)|2,V\rangle_s]\times[|1,H\rangle_i + \exp(i\phi_i)|2,V\rangle_i] \\ &\quad + [|2,H\rangle_s + \exp(i\phi_s)|3,V\rangle_s]\times[|2,H\rangle_i + \exp(i\phi_i)|2,V\rangle_i] \\ &= [|1,H\rangle_s|1,H\rangle_i + \exp(i\phi_i)|1,H\rangle_s|2,V\rangle_i] + \exp(i\phi_s)|2,V\rangle_s|1,H\rangle_i \\ &\quad + \exp[i(\phi_s+\phi_i)]|2,V\rangle_s|2,V\rangle_i + |2,H\rangle_s|2,H\rangle_i + \exp(i\phi_i)|2,H\rangle_s|3,V\rangle_i \\ &\quad + \exp(i\phi_s)|3,V\rangle_s|2,H\rangle_i + \exp[i(\phi_s+\phi_i)]|3,V\rangle_s|3,V\rangle_i \end{aligned} \quad (5)$$

By the coincidence counts in the second time slot, we can extract the fourth and fifth terms. As a result, we can obtain the following polarization entangled state as

$$|\Phi\rangle = |2,H\rangle_s|2,H\rangle_i + \exp[i(\phi_s+\phi_i)]|2,V\rangle_s|2,V\rangle_i \quad (6)$$

We assume that the response time of the Kerr effect is much less than the cavity round-trip time. Because of the Kerr nonlinearity of the optical device [10,11], strong pulses acquire an intensity-dependent phase shift during propagation. The interference of light pulses at the coupler introduces the superposition of light, which is entangled. Due to the polarization, states of light pulses are changed and converted while circulating in the delay circuit where the polarization entangled photon pairs can be generated. The entangled photons of the nonlinear ring resonator are separated to be the signal and the idler photons. A polarization angle adjustment device is used to investigate the orientation and the optical output intensity where the compensation, i.e. the measurement, is performed.

Generally, there are two pairs of possible polarization entangled photons, which are represented by the four polarization orientation angles as [0°, 90°] and [135°, 180°]. They can be formed by using a quarter wave plate after the polarization rotation device and the polarizing beam splitter. However, in practice, a continuously variable entangled photon can be generated, which introduces the possibility that a random entangled photon pair can be formed from the photon visibility. To generate the polarized photons, a rotatable polarizer is included in the system

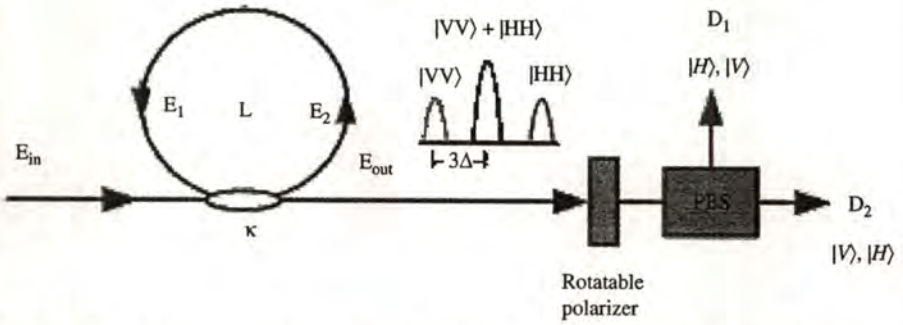

Fig. 2. A schematic of the entangled-photon generation system; PBS: Polarizing Beam Splitter and Ds: Detectors.

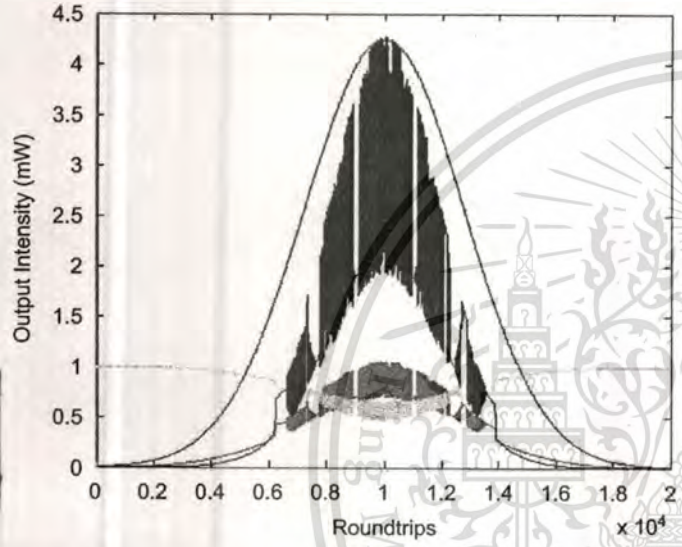

Fig. 3. The output characteristics of the chaotic signals, where (a) is the input signal (red), (b) the output signal (blue), (c) the polarized photon in horizontal mode (green) and (d) the vertical mode (yellow). (For interpretation of the references to colour in this figure legend, the reader is referred to the web version of this article).

after the ring device as shown in Fig. 2. The output polarized state is controlled by a rotatable polarizer, where the input azimuth angle is changed to obtain the required state. The randomly polarized light is formed from the specific angle by controlling the rotatable polarizer and the PBS. The two polarization modes ($|H\rangle$ and $|V\rangle$) are randomly formed and detected by the two detectors. By rotating the azimuth angles from 0 to 180°, the polarization entangled photon visibility is plotted and seen.

We assume that polarization rotation of light traveling through the optical device is represented by the rotation matrix (M):

$$M(\theta) = R(\theta)\,MR(-\theta) \tag{7}$$

where

$$R = \begin{bmatrix} \cos\theta & -\sin\theta \\ \sin\theta & \cos\theta \end{bmatrix}$$

where θ is the polarization azimuth angle.

The investigation of the output light characteristics within the ring device is described as follows: A Gaussian input pulse with peak power at 4.25 mW is input into the device via the input port. We use a ring device radius of 10 μm. To generate the polarized photon, where the nonlinear effects can be well performed, a chaotic oscillation is introduced into the micro-ring resonator. The parameters used are the coupling coefficient $\kappa = 0.02$–0.3, and the nonlinear refractive index $n_2 = 2.2 \times 10^{-15}$ $m^2\,W^{-1}$. The completed chaotic signals occur within the round-trips of 20,000 (time) as shown in Fig. 3, where (a) and (b) are the input (red line) and the output signals (blue), respectively. The projection of the output signals (c) and (d) via a polarization control unit are the polarized photon in horizontal (green) and vertical modes (yellow), respectively. Fig. 4 shows the output of the chaotic signals with different coupling constants, where (a) $\kappa = 0.3$, (b) $\kappa = 0.4$, (c) $\kappa = 0.5$ and (d) $\kappa = 0.7$. This can be formed by using the appropriate ring parameters, which were described by Yupapin and Suwancharoen [4].

3. Birefringence based sensor

When polarized light propagates in the optical device, the change in birefringence is introduced. This means the change in phase of the entangled photon pair occurs. The transvere walk-off produces a shift between the ordinary and the extraordinary modes, while the longitudinal walk-off introduces a time delay between horizontally and vertically polarized photons. The amount of walk-off depends on the location where the photon pairs are created within the device. This position is completely random due to the coherent nature of light in the optical device. To compensate for the longitudinal timing-walk-off effect, a polarization controller is recommended to ensure that the polarization rotation is the same on both photons from the entangled pair. In addition, a polarization rotation device is used to change the relative phase, ϕ, of the states of the polarized light. Because of the change in birefringence, tilting of the compensator (i.e. the rotatable device) allows application of a phase shift to the entangled states of the two entangled photons, which is given by [1]

$$|\psi\rangle_{12} = \frac{1}{\sqrt{2}}(|H\rangle_1 \otimes |V\rangle_2 + e^{i\phi}|V\rangle_1 \otimes |H\rangle_2) \tag{8}$$

From a sensing perspective, the walk-off entangled state parameters involved in the measurement are related to changes in applied physical parameters such as force, stress, strain, heat, pressure, etc. and optical device properties. However, the interesting parameters in this proposed systems are concerning the optical birefringence parameters, which can be given by

$$\Delta\phi = \frac{2\pi(n_x - n_y)L_w}{\lambda} \tag{9}$$

where $\Delta n = (n_x - n_y)$ is the optical birefringence, L_w is the entangled states walk-off length, and λ is the light source wavelength.

In principle, the movement of the signal and the idler from the optimum location introduces the walk-off length change, which can be compensated, i.e. measured. This effect is presented by the measurement parameter known as the walk-off length.

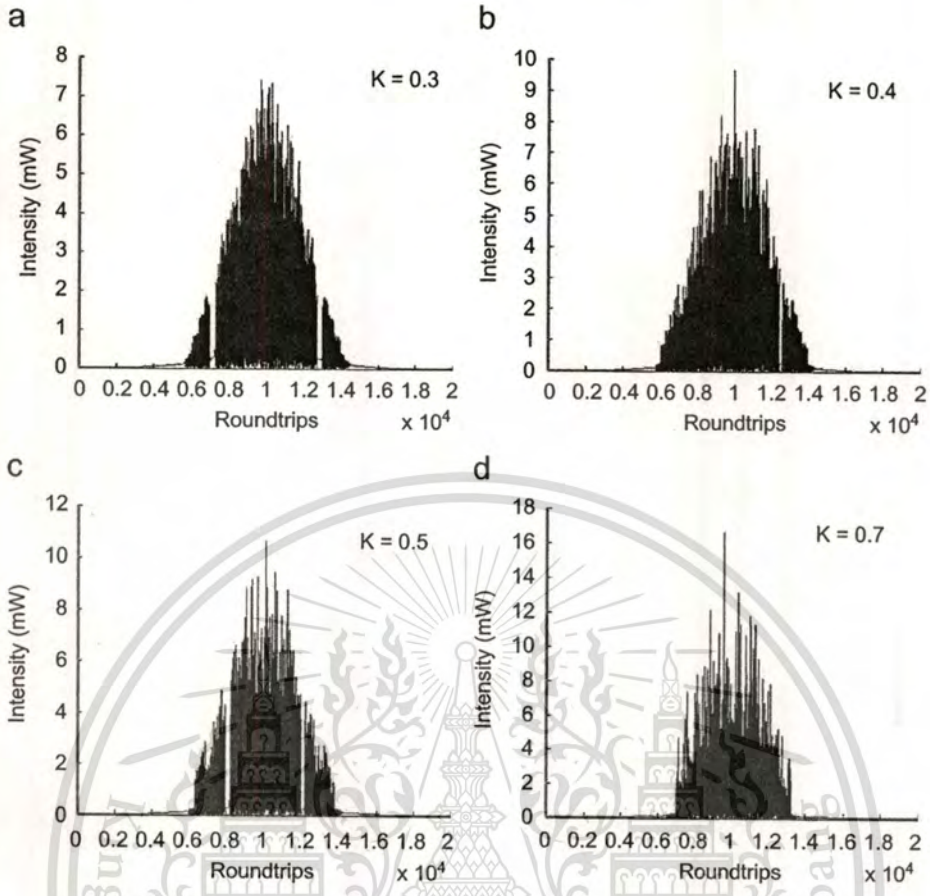

Fig. 4. The chaotic signals obtained when (a) $\kappa = 0.3$, (b) $\kappa = 0.4$, (c) $\kappa = 0.5$ and (d) $\kappa = 0.7$.

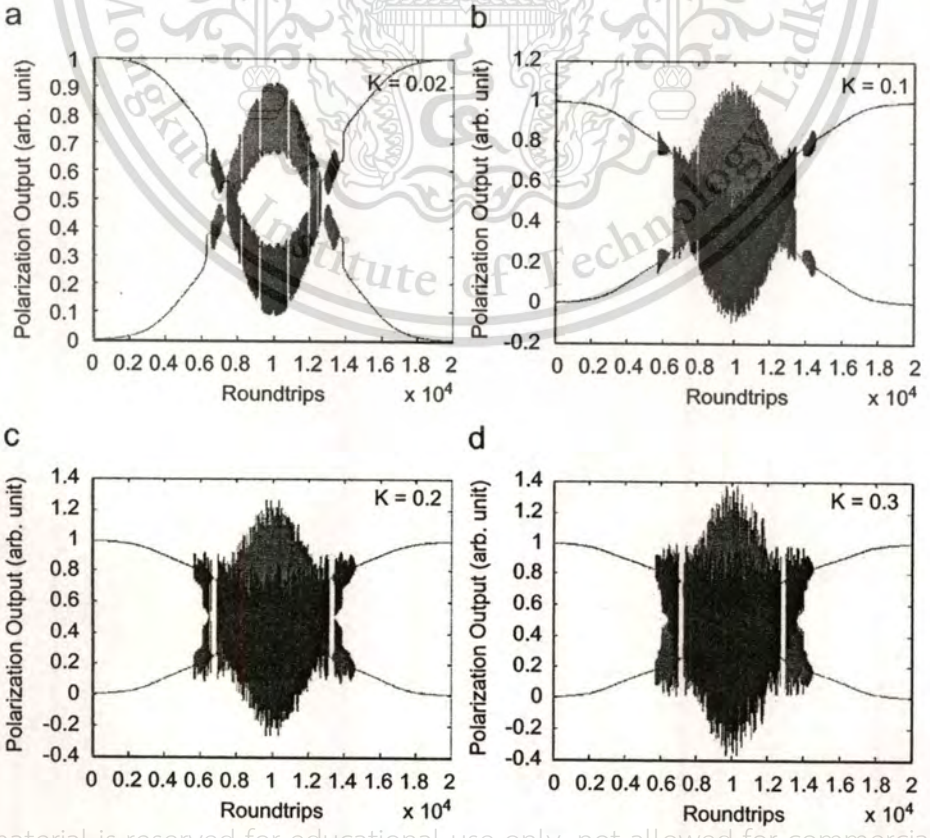

Fig. 5. Graph of the polarization output with different coupling coefficients, where green (top) and blue (bottom) represent horizontal and vertical polarized lights, respectively (a) $\kappa = 0.02$ (b) $\kappa = 0$, (c) $\kappa = 0.2$ and (d) $\kappa = 0.3$. (For interpretation of the references to colour in this figure legend, the reader is referred to the web version of this article).

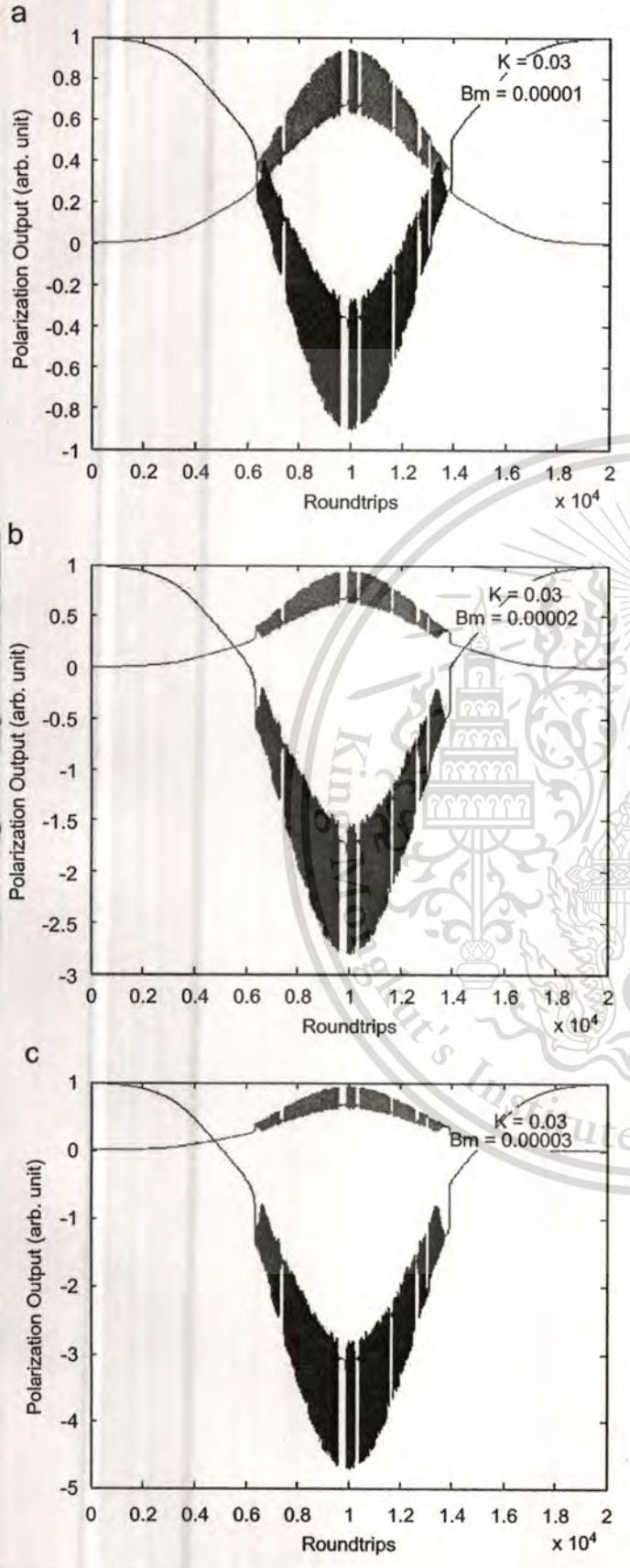

Fig. 6. Graph of the polarized photon with different modal birefringences [(Bm) = |nx−ny|], where green (top) and blue (bottom) represent the horizontal and the vertical polarized mode, respectively (a) $B_m = 1 \times 10^{-5}$, (b) $B_m = 2 \times 10^{-5}$ and (c) $B_m = 3 \times 10^{-5}$. (For interpretation of the references to colour in this figure legend, the reader is referred to the web version of this article).

The entangled photon visibility is randomly formed by a pair of signal and idler, which was described by Ref. [9]. The output photon projection can be described by using the matrix representation in Eq. (7). When the chaotic signal is generated, passing through the rotatable polarizer and polarizing beam splitter, the required azimuth angle is adjusted to obtain the specific orientation angle via the rotatable polarizer. The random entangled photon pair is split via a PBS and detected by the two detectors. In general, the entangled photon pairs may be formed by two different forms of the orientation angles (0°, 90°) or (135°, 180°), which is represented by light traveling into the optical components as described earlier. The entangled photon visibility is seen when the azimuth angle is rotated between 0 and 180°, where each peak power of the entangled photon pair is formed by each value of the maximum peak power at the specific orientation angle.

Fig. 5 shows a plot of one random azimuth angle of the output signal with different coupling coefficients, where (a) $\kappa = 0.02$, (b) $\kappa = 0$, (c) $\kappa = 0.2$ and (d) $\kappa = 0.3$. This shows that a good separation between horizontal (green) and vertical (blue) modes is seen when $\kappa = 0.02$. Fig. 6 shows the polarized output signal with different modal birefringences, where (a) $B_m = 1 \times 10^{-5}$, (b) $B_m = 2 \times 10^{-5}$ and (c) $B_m = 3 \times 10^{-5}$, where $[B_m = \Delta n = |n_x - n_y|]$. This shows that the change in modal birefringence causes a shift of the optimum entangled photon visibility, which is called the entangled photon timing walk-off. This can be compensated by adjusting the input polarizer to recover or obtain the optimum photon visibility. In practice, the required physical parameters can be applied to the micro-ring resonator, then the compensation of the shift in optimum entangled photon visibility can be made. This means that the relationship between walk-off length and phase of the polarized photon as in Eq. (9) is known.

The experimental result of our work using the same principle was published in Ref. [9]. It was shown that the optimum entangled photon visibility can be recovered (compensated) by rotating the polarizer angle, where the change in the entangled photon timing-walk-off in response to temperature changes was measured, shown in Fig. 7. Result obtained showed that the normalized optical intensity of the polarization output. The temperature ranged from 30 to 80 °C. In each measurement, light pulses are input into a polarizer and oriented, which was rotated from 0 to 180° before launching into the PBC. To recover the change in phase due to temperature change, the rotatable device before the polarizing beam splitter is adjusted. Then the measured orientation angle is noted and plotted relative to the change in

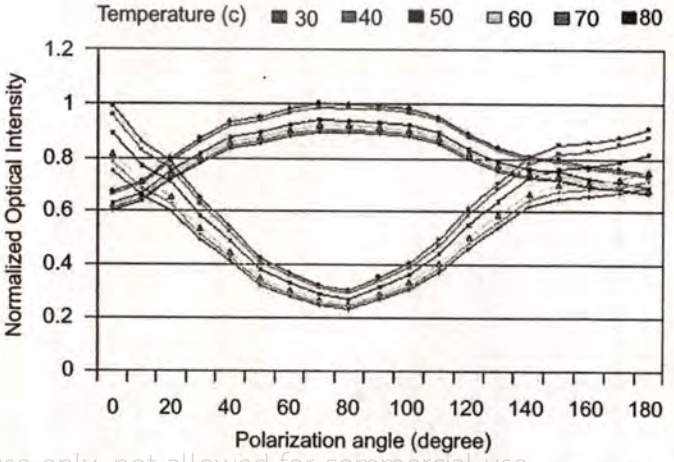

Fig. 7. Graph of the entangled-photon visibility and the polarization angles with thermal effects [9].

fiber birefringence (Δn, i.e. physical parameter). This means the entangled state walk-off is compensated.

4. Conclusion

We have demonstrated that the technique of the entangled photon walk-off compensation using a micro-ring resonator can be used to perform the birefringence-based sensing applications. The analysis of the entangled photon states generated within the ring device has been described. Two pairs of the orthogonal polarized modes can be formed and detected by using the external optical components incorporating the micro-ring device. Results obtained have shown that the use of the system for birefringence based sensing application is plausible, which is in good agreement with the experimental result.

References

[1] Yupapin PP. Fiber optic sensing applications using the entangled states walk-off compensations. Int J Light Electron Opt 2007.
[2] Grover R, Absil PP, Van V, Hryniewicz JV, Little BE, King O, et al. Vertically coupled GaInAsP–InP micro ring resonators. Opt Lett 2001;26:506–9.
[3] Yupapin PP, Suwanchroen W. A novel technology for mobile telephone networks and security. In: Harper Alvin C, Buress Raymond V, editors. Mobile telephones: networks, applications, and performance. New York: Nova Science Publishers; 2008. p. 265–74.
[4] Yupapin PP, Suwancharoen W. Chaotic signal generation and cancellation using a micro ring resonator incorporating an optical add/drop multiplexer. Opt Commun 2007;280:343–9.
[5] Yupapin PP, Khunnam W, Suchat S. The entangled photons generation system using weak light in fiber optic and timing-walk-off compensation. Int J Quantum Inf 2007;5:805–15.
[6] Yupapin PP, Suchat S. Entangle photon generation using fiber optic Mach–Zehnder interferometer incorporating nonlinear effect in a fiber ring resonator. J Nanophotonics 2007;1:013504.
[7] Sripakdee C, Sarpat K, Suwancharoen W, Yupapin PP. Entangled photon generation in a nonlinear micro ring resonator for quantum key distribution use. In: Proceedings in SmarMat-08 & IWOFM-2, Chiang Mai, 2008.
[8] Fietz C, Shvets G. Nonlinear polarization conversion using micro ring resonators. Opt Lett 2007;32:1683–5.
[9] Suchat S, Khunnam W, Yupapin PP. Entangled photons generation and recovery using a fiber ring resonator incorporating an erbium doped fiber amplifier. Opt Eng 2008;47:100502-1-5.
[10] Silberhorn Ch, Lam PK, Weib O, Konig F, Korolkova N, Leuchs G. Generation of continuous variable Einstein–Podolsky–Rosen entanglement via the Kerr nonlinearity in an optical fiber. Phys Rev Lett 2001;86:4267–70.
[11] Ogusu K, Shigekuni H, Yokota. Dynamic transmission properties of a nonlinear fiber ring resonator. Opt Lett 1995;20:2288–90.

ARTICLE IN PRESS

Available online at www.sciencedirect.com

ScienceDirect

Optik ▮ (▮▮▮▮) ▮▮▮–▮▮▮

Optik Optics

www.elsevier.de/ijleo

Entangled photon generation in a nonlinear microring resonator for birefringence-based sensing applications

P.P. Yupapin*, P. Yabosdee, P. Phiphithirankarn

Advanced Research Center for Photonics, Department of Applied Physics, Faculty of Science, King Mongkut's Institute of Technology Ladkrabang, Bangkok 10520, Thailand

Received 7 March 2008; accepted 12 July 2008

Abstract

This paper proposes a new concept of birefringence-based sensor using the entangled photon timing walk-off compensation. The superposition of nonlinear light known as four-wave mixing is introduced by the Kerr nonlinear effects type within the ring device. The possible two entangled photon pairs are randomly generated using the polarization control unit. Results obtained have shown that the entangled state walk-off of light traveling within the ring device can be compensated. This means the changes in walk-off parameters can be relatively measured to the changes in the applied physical parameters. The potential of using such a proposed system for birefringence-based sensor applications is plausible and discussed.

Keywords: Nonlinear microring resonator; Birefringence sensor; Entangled photon

Yupapin [1] has shown a concept of an ultrahigh measurement resolution method using polarized photon in a fiber optic ring resonator. He has concluded that the shift in optimum entangled photon visibility can be compensated by the appropriate walk-off length, where the measurement resolution is increased by the order of the change in material birefringence. However, the structure of fiber optic system becomes a problem due to the external environment suffering. Alternatively, an optical microring resonator has been widely investigated both in theoretical and in experimental works. It is found that the device scale is dramatically decreased, where the device scale of a few microns is fabricated and available [2]. One of the promising application aspects is that it can be fabricated to process the signal processing within the small device, where the secure message, i.e. security, can be performed. For instance, techniques such as chaos [3], quantum entanglement [4] and chaotic quantum [5] have shown the potential of applications. Recently, Fietz and Shvets [6] have reported that the polarized entangled photons can be generated by using a microring device, which is associated with the practical devices, and have been fabricated [7]. Khunnan and Yupapin [8] have shown the entangled photon recovery, i.e. regeneration using fiber optic ring resonator incorporating an EDFA, which is useful for long distance link. However, the problem of polarization dispersion causes the entangled photon, a problem called timing walk-off [9], which has become a problem in the recovery process. In this paper, we design the microring device to generate the polarized entangled photons for sensing applications. The entangled photon

*Corresponding author. Tel.: +66 2 3264339; fax: +66 2 3264354.
E-mail address: kypreech@kmitl.ac.th (P.P. Yupapin).
URL: http://URL://www.kmitl.ac.th/~arcp (P.P. Yupapin).

0030-4026/$ - see front matter © 2008 Elsevier GmbH. All rights reserved.
doi:10.1016/j.ijleo.2008.07.024

Please cite this article as: P.P. Yupapin, et al., Entangled photon generation in a nonlinear microring resonator for birefringence-based sensing applications, Opt. Int. J. Light Electron. Opt. (2008), doi:10.1016/j.ijleo.2008.07.024

generation and behaviors within the proposed device are analyzed and discussed. The device parameters are simulated associated with the practical device. Results obtained have shown that it is a good potential of using such a device for birefringence-based sensing applications, where the measurement of physical parameters such as temperature, pressure, and moisture is plausible. The ultrahigh resolution in terms of walk-off length and material birefringence is described.

A schematic diagram of a ring device is as shown in Fig. 1, when light from a monochromatic light source is launched into a ring resonator with a constant light field amplitude (E_0) and random phase modulation (ϕ_0) as a function of time (t), which results in temporal coherence degradation. Hence, the input light field (E_{in}) can be expressed as

$$E_{in}(t) = E_0 \exp^{j\phi_0(t)}. \tag{1}$$

We assume that the nonlinearity of the optical ring resonator is of the Kerr-type, i.e. the refractive index is given by

$$n = n_0 + n_2 I = n_0 + \left(\frac{n_2}{A_{eff}}\right) P, \tag{2}$$

where n_0 and n_2 are the linear and nonlinear refractive indices, respectively. I and P are the optical intensity and optical field power, respectively. The effective mode core area of the device is A_{eff}.

Thus, the normalized output light of the system, as shown in Fig. 2, can be expressed by

$$\left|\frac{E_{out}(t)}{E_{in}(t)}\right|^2 = (1-\gamma) \times \left[1 - \frac{(1-(1-\gamma)x^2)\kappa}{(1-x\sqrt{1-\gamma}\sqrt{1-\kappa})^2 + 4x\sqrt{1-\gamma}\sqrt{1-\kappa}\sin^2(\phi/2)}\right]. \tag{3}$$

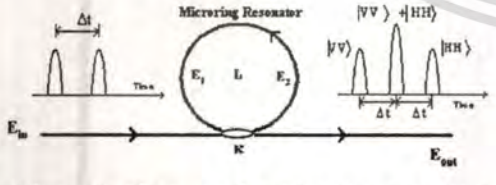

Fig. 1. Schematic diagram of a microring resonator with a coupling part of a microring resonator.

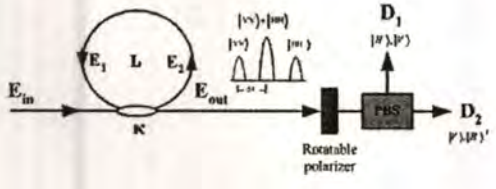

Fig. 2. A schematic of the entangled photon generation system. PBS: polarizing beam splitter, Ds: detectors.

A close examination of Eq. (3) indicates that a ring resonator in the particular case is very similar to a Fabry–Perot cavity, which has an input and output mirror with field reflectivity, $1-\kappa$, and a fully reflecting mirror, where n_0 and n_2 are the linear and nonlinear refractive indices, the coupling coefficient is κ. Here, $x = \exp^{-\alpha L/2}$ represents the one round-trip losses coefficient, $\phi_0 = kLn_0$ and $\phi_{NL} = kLn_2|E_1|^2$ are the linear and nonlinear phase shifts and $k = 2\pi/\lambda$ is the wave propagation constant in vacuum.

This nonlinear behavior of light traveling in a single-ring resonator is described as follows. When the parameters of the system are fixed to $\lambda_0 = 1.55\,\mu m$, $n_0 = 3.34$, $A_{eff} = 50\,\mu m^2$, where the waveguide (ring resonator) loss is $\alpha = 0.5\,dB\,mm^{-1}$. This practical bending loss of the waveguide fabricated by InGaAsP/InP is confirmed by Ref. [3], where the propagation loss is as low as $1.3 \pm .02\,dB\,mm^{-1}$ at $1.55\,\mu m$, the fractional coupler intensity loss is $\gamma = 0.1$ and $R_1 = 10\,\mu m$. The coupling coefficient of the coupler is fixed to $\kappa = 0.02$–0.3. The nonlinear refractive index used is $n_2 = 2.2 \times 10^{-15}\,m^2\,W^{-1}$, and the data of 20,000 iterations of roundtrips inside the optical microring are plotted. We assume that $\phi_L = 0$ for simplicity; however, the change in phase slightly alters the optical output, which means the dispersion can be neglected when resonant output occurs. In general, the input pulse can be a single pulse or pulse trains, where the output pulses after some roundtrips with random polarization are as shown in Fig. 1. H and V represent the horizontal and vertical polarization components, respectively.

To generate the polarized photons, the rotatable polarizer is employed into the system after the ring device as shown in Fig. 2. The output polarized state is controlled by a rotatable polarizer, where the input azimuth angle is changed to obtain the required state. Randomly polarized light forms the specific angle by controlling the rotatable polarizer and the polarizing beam splitter (PBS). The two orthogonal polarized modes (H and V) are performed and detected by the two detectors. By rotating the azimuth angles from 0° to 180°, the polarization-entangled photon visibility is plotted and seen.

We assume that the polarization rotation of light traveling along the optical devices is represented by the rotation matrix (**M**) as in Eq. (4):

$$M(\theta) = R(\theta)MR(-\theta), \tag{4}$$

where

$$R = \begin{bmatrix} \cos\theta & -\sin\theta \\ \sin\theta & \cos\theta \end{bmatrix}$$

and θ is the polarization azimuth angle.

Please cite this article as: P.P. Yupapin, et al., Entangled photon generation in a nonlinear microring resonator for birefringence-based sensing applications, Opt. Int. J. Light Electron. Opt. (2008), doi:10.1016/j.ijleo.2008.07.024

For instance, a horizontal linear polarizer $= \begin{bmatrix} 1 & 0 \\ 0 & 0 \end{bmatrix}$, a vertical linear polarizer$= \begin{bmatrix} 0 & 0 \\ 0 & 1 \end{bmatrix}$, a linear polarizer at $\theta = \begin{bmatrix} \cos^2\theta & \cos\theta\sin\theta \\ \cos\theta\sin\theta & \sin^2\theta \end{bmatrix}$.

Generally, there are two pairs of possible polarization-entangled photons, which are represented by the four polarization orientation angles as [0°, 90°] and [135°, 180°]. They can be formed by using the optical component called the polarization rotatable device and PBS.

When polarized light propagates in the fiber optic, the change in birefringence is introduced. This means the change in phase of the entangled photon pair has occurred. Here the transversal walk-off produces a shift between the ordinary and extraordinary, while the longitudinal walk-off introduces a time delay between horizontally and vertically polarized photons. The amount of walk-off depends on the location where the photon pairs are created within the fiber. This position is completely random due to the coherent nature of light in fiber optic. To compensate the longitudinal timing walk-off effect, a polarization controller is recommended to ensure that the polarization rotation is the same on both photons from the entangled pair. Additionally, the compensator fiber is used to change the relative phase ϕ of the states of polarized light. Because of the change in birefringence, the tilting of the compensator allows one to apply a phase shift to the entangled states of the two entangled photons, which is given by Eq. (5) as [1]

$$|\psi\rangle_{12} = \frac{1}{\sqrt{2}}(|H\rangle_1 \otimes |V\rangle_2 + e^{i\phi}|V\rangle_1 \otimes |H\rangle_2). \quad (5)$$

In applications, the walk-off entangled state parameters involved in the measurement are related to the changes in the applied physical parameters such as force, stress, strain, heat, pressure, etc. and the fiber optic properties. However, the interested parameters in this proposed systems concern the fiber optic birefringence parameters, which can be given by

$$\Delta\phi = \frac{2\pi(n_x - n_y)L_w}{\lambda}, \quad (6)$$

where $\Delta n = (n_x - n_y)$ is the fiber optic birefringence, L_w is the entangled states walk-off length and λ is the light source wavelength.

The investigation of the output light characteristics within the ring device is described as follows. A Gaussian input pulse with peak power at 4.25 mW is input into the device via the input port. We use a ring device radius of 10 μm. To generate the optimum possibility of the four-wave mixing (i.e. superposition) of polarized light, where the nonlinear effect can be well performed, chaotic oscillation is introduced into the system. The parameters used are the coupling coefficient; $\kappa = 0.02$–0.3, and the nonlinear refractive index; $n_2 = 2.2 \times 10^{-15}\,m^2W^{-1}$. The completed chaotic signals occur within the roundtrips of 20,000 as shown in Fig. 3. Here, (a) is the input signal (red line), (b) the output signal (blue), (c) the quantum chaotic signal in the horizontal mode (green) and (d) the vertical signal (yellow). In principle, the quantum chaotic behaviors can be described using the matrix representation in Eq. (4). When the chaotic signal is generated, it passes through the rotatable polarizer and the PBS. The required azimuth angle is adjusted to obtain the specific orientation angle via the rotatable polarizer. The random entangled photon pair is split via a PBS and detected by the two detectors. In general, the entangled photon pairs may be formed by two different forms of orientation angles [(0°, 90°) or (135°, 180°)], which is represented by light traveling into the optical components as described earlier.

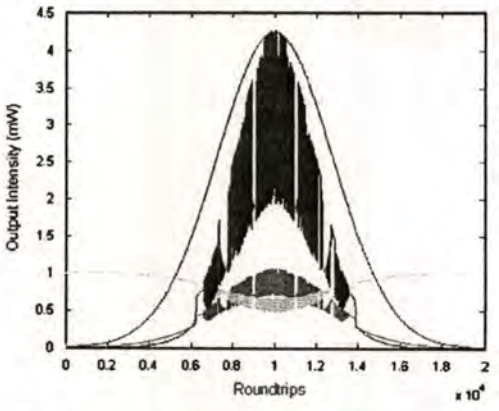

Fig. 3. The output characteristics of the quantum chaotic signals, where (a) is the input signal (red), (b) the output signal (blue), (c) the quantum chaotic signal in the horizontal mode (green) and (d) the vertical signal (yellow).

The entangled photon visibility is seen when the azimuth angle is rotated between 0° and 180°, where each peak power of the entangled photon pair is formed by each value of the maximum peak power at the specific orientation angle. In this case, the generation of simultaneous two pairs of entangled photons is plausible, i.e. four entangled photon states, where the device called the quarter wave plate is required into the system before each detector.

Fig. 4 shows the output of the chaotic signals with different coupling constants, where (a) $\kappa = 0.3$, (b) $\kappa = 0.4$, (c) $\kappa = 0.5$ and (d) $\kappa = 0.7$. This can be formed by using the appropriate ring parameters, which was well-described by Yupapin and Suwancharoen [3]. Fig. 5 shows the plot of one random azimuth angle of the quantum chaotic output with different coupling coefficients, where (a) $\kappa = 0.02$, (b) $\kappa = 0$, (c) $\kappa = 0.2$ and (d) $\kappa = 0.3$, and it also shows the good separation

Please cite this article as: P.P. Yupapin, et al., Entangled photon generation in a nonlinear microring resonator for birefringence-based sensing applications, Opt. Int. J. Light Electron. Opt. (2008), doi:10.1016/j.ijleo.2008.07.024

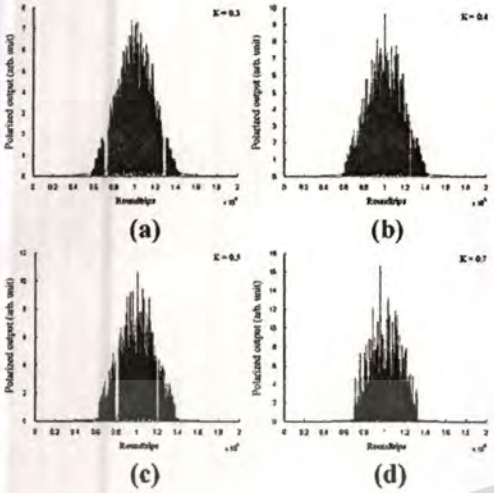

Fig. 4. The output of the chaotic signals, where (a) $\kappa = 0.3$, (b) $\kappa = 0.4$, (c) $\kappa = 0.5$ and (d) $\kappa = 0.7$.

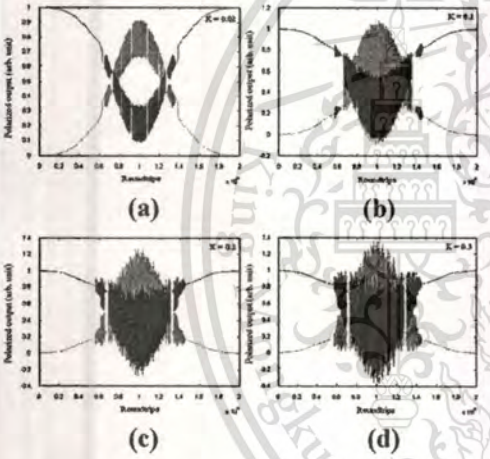

Fig. 5. Plot of the quantum chaotic output signal with different coupling coefficients, where (a) $\kappa = 0.02$, (b) $\kappa = 0$, (c) $\kappa = 0.2$ and (d) $\kappa = 0.3$.

between horizontal (green) and vertical (yellow) modes, when $K = 0.02$. Fig. 6 shows the simulation output of the quantum chaotic signals with different modal birefringence [(Bm) = $|n_x - n_y|$], where (a) Bm = 1×10^{-5}, (b) Bm = 2×10^{-5} and (c) Bm = 3×10^{-5}. Thus it is seen that the change in modal birefringence causes the shift of the optimum entangled photon visibility, which is called the entangled photon timing walk-off. This can be compensated by adjusting the input polarizer (i.e. the azimuth angle) to recovery or obtain the optimum photon visibility. In application, the required physical parameters can be performed on the sensing device (a microring resonator). The compensation of the shift in optimum entangled photon visibility can be made. This means that the relationship between walk-off length and phase of the polarized photon as in Eq. (6)

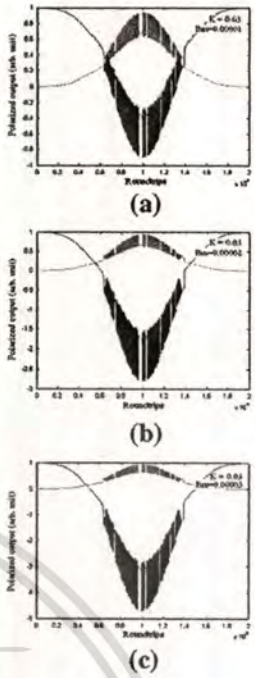

Fig. 6. Simulation output of the quantum chaotic signals with different modal birefringence [(Bm) = $|n_x - n_y|$], where (a) Bm = 1×10^{-5}, (b) Bm = 2×10^{-5} and (c) Bm = 3×10^{-5}.

is known. In conclusion, the quantum chaotic signal generated by light traveling in the microring resonator is simulated. The analysis of the entangled photon states generated within the ring device can be shown. Two pairs of orthogonal polarized modes can be formed and detected using the optical components incorporating the microring device. Simulation results obtained have shown that the use of the system for birefringence-based sensing application is plausible.

We would wish to thank Dr. S. Suchat and Dr. N. Pornsuwancharoen from Department of Physics, Faculty of Science and Technology, Thammasat University, and Department of Electronics, Faculty of Engineering, Rajamangala University of Technology, Isan, Thailand, respectively, for their useful comments.

References

[1] P.P. Yupapin, Fiber optic sensing applications using the entangled states walk-off compensations, Int. J. Light Electron Opt. (2007).

[2] R. Grover, P.P. Absil, V. Van, J.V. Hryniewicz, B.E. Little, O. King, L.C. Calhoun, F.G. Johnson, P.-T. Ho, Vertically coupled GaInAsP–InP microring resonators, Opt. Lett. 26 (2001) 506.

[3] P.P. Yupapin, W. Suwancharoen, Chaotic signal generation and cancellation using a micro ring resonator

incorporating an optical add/drop multiplexer, Opt. Commun. 280 (2007) 343.
[4] P.P. Yupapin, W. Khunnam, S. Suchat, The entangled photons generation system using weak light in fiber optic and timing walk-off compensation, Int. J. Quant. Inform. 5 (2007) 805.
[5] C. Sripakdee, K. Sarpat, W. Suwancharoen, P.P. Yupapin, Entangled photon generation in a nonlinear micro ring resonator for quantum key distribution use, in: Proceedings of the Smartmat-08 & IWOFM-2, Chiang Mai, 2008.
[6] C. Fietz, G. Shvets, Nonlinear polarization conversion using micro ring resonstors, Opt. Lett. 32 (2007) 1683.
[7] H. Takesue, K. Inoue, O. Tadanaga, Y. Nishida, M. Asobe, Generation of pulsed polarization-entangled photon pairs in a 1.55-μm band with a periodically poled lithium niobate waveguide and an orthogonal polarization delay circuit, Opt. Lett. 30 (2005) 293.
[8] W. Khunnam, P.P. Yupapin, An investigation of the entangled photon walk-off compensation generated by a fiber ring resonator, Int. J. Light Electron Opt. (2008) in press, doi:10.1016/j.ijleo.2008.02.025.
[9] P. Trojek, Ch. Schmid, M. Bourennane, H. Weinfurter, Compact source for polarization entangled photon pairs, Opt. Exp. 12 (2004) 276.

Please cite this article as: P.P. Yupapin, et al., Entangled photon generation in a nonlinear microring resonator for birefringence-based sensing applications, Opt. Int. J. Light Electron. Opt. (2008), doi:10.1016/j.ijleo.2008.07.024

ARTICLE IN PRESS

Available online at www.sciencedirect.com

ScienceDirect

Optik ▮ (▮▮▮▮) ▮▮▮–▮▮▮

Optik Optics

www.elsevier.de/ijleo

An investigation of quantum–chaotic signals generation using a fiber ring resonator and an add/drop multiplexer

P. Chunpang[a], P. Piphithirankarn[b], P.P. Yupapin[b,*]

[a]*Department of Physics, Faculty of Science, Mahasarakham University, Mahasarakham 44150, Thailand*
[b]*Advanced Research Center for Photonics, Department of Applied Physics, Faculty of Science, King Mongkut's Institute of Technology, Ladkrabang, Bangkok 10520, Thailand*

Received 1 July 2008; accepted 14 September 2008

Abstract

We successfully generate the double security using a fiber ring resonator incorporating an add/drop device, whereas the quantum–chaotic encoding of light in a single fiber ring resonator is constructed. In the experiment, the nonlinear Kerr effects in the fiber ring resonator induced the chaotic wave form within the fiber ring resonator, which could be used to scramble or encode into the original signals. The laser input power used was 15 mW, with a fiber ring radius of 50 cm. We found that the double security can be formed, where the randomly polarized photons could be controlled by using the polarization controller and observed.

Keywords: Quantum encoding; Chaotic signals; Fiber ring resonator; Add/drop filter; Signal security

1. Introduction

Yupapin et al. [1] have reported the interesting simulation results of the chaotic behaviors of light within a fiber ring resonator. The chaotic behaviors can be formed within a fiber ring resonator by using the appropriate parameters such as ring radius, optical input power and coupling coefficient. Whereas the fiber lengths used were varied from few to hundred meters, with the coupling optical power of 10–15 mW. However, several research works have proposed the use of chaotic behaviors in various applications. For instance, chaotic signals can be used to form the digital encoding [2], where the retrieval signals in either analog or digital signals can be performed [3]. Furthermore, the quantum codes (bits) can be generated by using the fiber ring resonator and polarization control devices [4,5]. Recently, the concept of quantum–chaotic signal generation proposed by Yupapin and Chunpang [6], have reported the schematic concept where the double security can be performed by using the fiber ring resonator. In principle, the chaotic noisy signals can be generated by the nonlinear Kerr type effects, while the quantum bits can be formed by using the polarized photons with the polarization control arrangement. However, the relationship between the input power and fiber ring radius has become the key condition of this phenomenon. In this work, we have experimentally investigated the use of double encoding by using quantum and chaotic codes. The chaotic noisy signals can be recovered by using the fiber optic add/drop filter, which is well described in Ref. [7]. The entangled photon state detection is observed and the quantum codes formed by using fiber ring resonator and polarizing control devices, which is confirmed by Ref. [8]. Results

*Corresponding author.
E-mail address: kypreech@kmitl.ac.th (P.P. Yupapin).

0030-4026/$ - see front matter © 2008 Elsevier GmbH. All rights reserved.
doi:10.1016/j.ijleo.2008.09.023

Please cite this article as: P. Chunpang, et al., An investigation of quantum–chaotic signals generation using a fiber ring resonator and an add/drop multiplexer, Opt. Int. J. Light Electron. Opt. (2009), doi:10.1016/j.ijleo.2008.09.023

obtained have confirmed in good agreement with the concept paper in Ref. [6]. In practice, the required signals could be retrieved from the chaotic noisy signals by using add/drop multiplexing device. The polarized photon is formed and detected by using the polarization control unit and detectors. The initial quantum codes (qubits) can be generated and formed by Alice, where the corrected codes i.e. qubits in the network can be confirmed by Bob. Results obtained have shown the potential application that the use of double security via quantum–chaotic codes is plausible. We have especially concentrated on the experimental work, however, the theoretical background of the chaotic signal generation and add/drop device is reviewed.

2. Operating principle

Consider a fiber optic ring resonator (FORR) configuration is depicted in Fig. 1, which is constructed by a sing mode fiber length and a 2×2 optical coupler. The circumference of the fiber ring is L. For convenience of analysis, we assume the complex electric field at each port as shown in Fig. 1. $E_{in}(t)$ is the incoming light field of an input port and the transmitted light field to the output port is $E_{out}(t)$. While the rest of the fields $E_1(t)$ and $E_2(t)$ are the circulated fields inside the fiber ring.

Here, the input light is assumed to be monochromatic with constant amplitude and random phase modulation which results in temporal coherence degradation. Hence, the input light field can be expressed as

$$E_{in}(t) = E_0 \exp^{j\phi_0(t)}. \tag{1}$$

According to light transmission theory in linear optical systems, we obtain the relations between the electric fields $E_1(t)$, $E_2(t)$, $E_{in}(t)$ and the output field $E_{out}(t)$ as following equations:

$$E_1(t) = \sqrt{1-\gamma}[\sqrt{1-\kappa}E_2(t) + j\sqrt{\kappa}E_{in}(t)], \tag{2}$$

$$E_{out}(t) = \sqrt{1-\gamma}[\sqrt{1-\kappa}E_{in}(t) + j\sqrt{\kappa}E_2(t)], \tag{3}$$

$$E_2(t) = \exp^{-(\alpha L/2)-j\phi}E_1(t). \tag{4}$$

After one round-trip the electric field E_1 makes the nonlinearity inside the FORR is due to changes in the refractive index with optical power. Here, the power dependence of refractive index is responsible for the

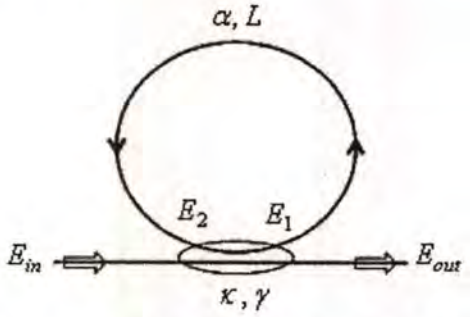

Fig. 1. Schematic of a fiber optic ring resonator with a single mode directional coupler.

Kerr effect and the refractive index can be written as

$$n = n_0 + n_2 I = n_0 + \left(\frac{n_2}{A_{eff}}\right)|E_1(t)|^2, \tag{5}$$

where n_0 and n_2 are the linear and nonlinear refractive indexes, respectively. I is the optical field intensity and the effective mode core area of the fiber is A_{eff}. Therefore, the circulated field E_2 has a phase shift including linear and nonlinear parts as

$$\phi = \phi_0 + \frac{\pi}{2} + \Delta\phi_{NL}, \tag{6}$$

where $\phi_0 = kLn_0$ and $\phi_{NL} = kLn_2|E_1|^2$ are the linear and nonlinear phase shift, $k = 2\pi/\lambda$ is the wave propagation number in vacuum. Substituting these parameters in Eq. (6) and then can be written as

$$\phi(t) = \phi_0 + \frac{\pi}{2} + \frac{2\pi n_2 L}{\lambda A_{eff}}|E_1(t)|^2. \tag{7}$$

Generally, the occurring of nonlinear behavior of light within a FORR depends on the relationship between nonlinear refractive index (n_2) and the input optical field. However, the nonlinear refractive index of a single mode fiber is a small value, therefore, the intense optical field or small ring radius is required to obtain the nonlinear output. Simulation results have been confirmed by Yupapin et al. [1], where the fiber ring length used is 80 m, the input optical power is 15 mW. In this work, we have reduced the ring radius to make a good result for future investigation with micro ring device. The ring length used is 15 cm which is formed as a ring resonator. The available optical power used is 10 mW. To retrieve the signals from the chaotic noise, we propose to use the add/drop device with the appropriate parameters. This is given in detail as followings. The two complementary optical circuits of ring-resonator add/drop filters can be given by [9],

$$\left|\frac{E_t}{E_{in}}\right|^2 = \frac{(1-\kappa_1) - 2\sqrt{1-\kappa_1}\cdot\sqrt{1-\kappa_2}e^{-(\alpha/2)L}\cos(k_n L) + (1-\kappa_2)e^{-\alpha L}}{1 + (1-\kappa_1)(1-\kappa_2)e^{-\alpha L} - 2\sqrt{1-\kappa_1}\cdot\sqrt{1-\kappa_2}e^{-(\alpha/2)L}\cos(k_n L)} \tag{8}$$

and

$$\left|\frac{E_d}{E_{in}}\right|^2 = \frac{\kappa_1\kappa_2 e^{-(\alpha/2)L}}{1 + (1-\kappa_1)(1-\kappa_2)e^{-\alpha L} - 2\sqrt{1-\kappa_1}\cdot\sqrt{1-\kappa_2}e^{-(\alpha/2)L}\cos(k_n L)} \tag{9}$$

Please cite this article as: P. Chunpang, et al., An investigation of quantum–chaotic signals generation using a fiber ring resonator and an add/drop multiplexer, Opt. Int. J. Light Electron. Opt. (2009), doi:10.1016/j.ijleo.2008.09.023

where E_t and E_d represents the optical fields of the throughput and drop ports, respectively. $\beta = kn_{eff}$ is the propagation constant, n_{eff} is the effective refractive index of the waveguide and the circumference of the ring is $L = 2\pi R$, here R is the radius of the ring. In the following, new parameters will be used for simplification: $\phi = \beta L$ is the phase constant. The chaotic noise cancellation can be managed by using the specific parameters of the add/drop device, which the required signals can be retrieved by the specific cases. K_1 and K_2 are the coupling coefficients of add/drop filters, $k_n = 2\pi/\lambda$ is the wave propagation number in a vacuum, and the waveguide (ring resonator) loss is $\alpha = 0.5\,\mathrm{dB\,mm^{-1}}$. The fractional coupler intensity loss is $\gamma = 0.1$. In the case of add/drop device, the nonlinear refractive index is neglected.

3. Experimental results and discussion

The experimental setup of the quantum–chaotic signal generation using a fiber ring resonator incorporating an add/drop device is as shown in Fig. 2. The optical tunable light source with large tuning range is employed to obtain the input pulse at the required wavelength. The optical field input (E_{in}) is input into the system. In Fig. 2, a laser pulse with wavelength 1520 nm at the output peak power of 10 mW is injected into the system via a fiber coupler with coupling ratio of 90/10. One arm of the coupler is connected to a 90% coupler output port to form a ring resonator. The fiber ring length used is 15 cm, for the optimum chaotic signal generation. One half of the optical power is coupled by an add/drop device via a 3 dB fiber coupler, where the rest of the power is input into the throughput port (through port). The filtering characteristics of the add/drop device allows the required signal falling on the detector and optical spectrum analyzer via the 3 dB coupler. In general, the add port is able to perform the multiplexing function. However, it was not used in this experiment. Finally, the throughput port is connected to the polarization control devices and detectors. The chaotic signal obtained is shown in Fig. 3(a), where the center wavelength is 1530 nm with the output peak power of −1.68 dB m. The chaotic noise floor level is about −37 dB m. In Fig. 3(b), the retrieved signal is obtained by using the add-drop filter. The center wavelength is 1530 nm with the output peak power of 2.89 dB m.

The other part, the change in phase of the polarized photon is controlled by using the polarization controller (PC). The adjusting of the polarization angle from 0 to 360°, this can be performed by tilting the PC, which caused the change of both entangled states and optical output intensity. To confirm the existence of entangled states, then each photon was input into a polarizer and orientation from 0 to 180° before launching into the PBC. The output photons were detected by using the avalanche photodiodes (APDs). The polarized photon visibility is plotted and shown in Fig. 4, where the noise floor occurs due to the chaotic generated signals at the first fiber ring resonator.

After a certain number of roundtrips, the resonant noisy chaotic signals are observed as shown in Fig. 3(a). The nonlinear Kerr type induces the randomly superposed four-wave mixing of light pulse within the fiber ring resonator. The operating wavelength is 1520 nm as shown in Fig. 3. The original waveform (i.e. input signal) is retrieved from the chaotic signals as shown in Fig. 3(b), whereas the chaotic signals are cancelled when the signal is coupled into the add/drop device. In applications, the chaotic signals could be either analog or digital forms. However, the use of digital one is more useful than the analog one. The throughput port output is coupled into the add/drop device, the other part is formed the polarized photon. The polarized photons were formed by using the PC. At this point, the random quantum codes (qubits) can be formed by using

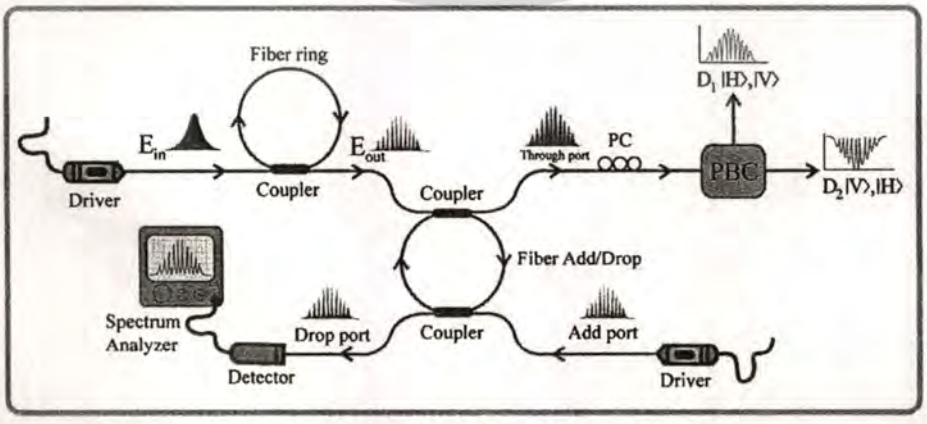

Fig. 2. A schematic of the quantum–chaotic signal generation system; PC: polarization controller, PBC: polarization beam coupler, Ds: detectors.

Please cite this article as: P. Chunpang, et al., An investigation of quantum–chaotic signals generation using a fiber ring resonator and an add/drop multiplexer, Opt. Int. J. Light Electron. Opt. (2009), doi:10.1016/j.ijleo.2008.09.023

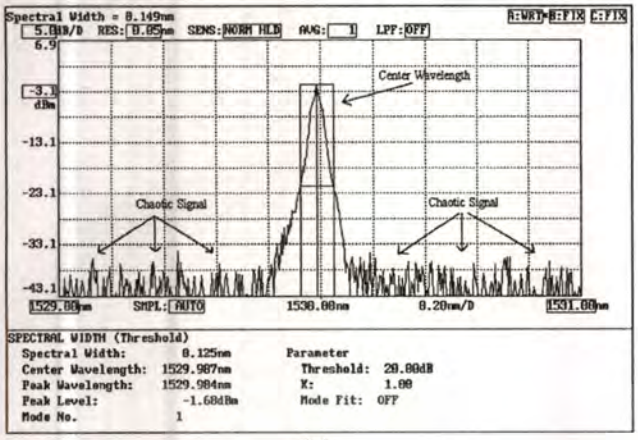

(a)

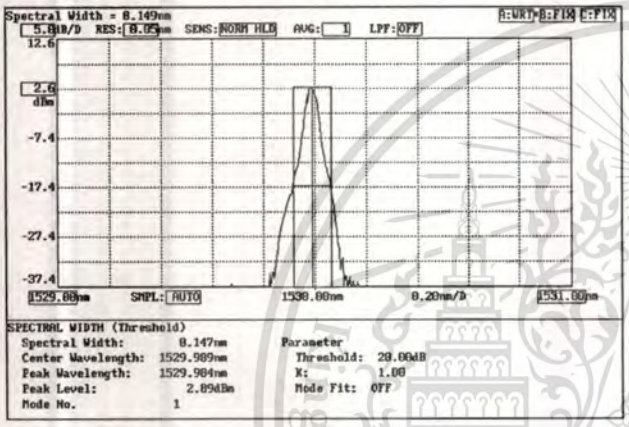

(b)

Fig. 3. Spectrum output of the experimental results obtained at two different ports, (a) a throughput port and (b) a drop port.

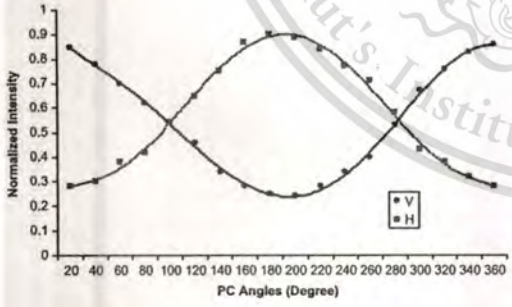

Fig. 4. Graph of the normalized output of the polarized photon at the throughput port.

horizontal (H) or vertical (V) polarization to form the random logic codes "0" or "1". The initial bits can be performed and recognized by Alice, the decode bits can be formed by Bob. The secret codes can be recovered by Alice and Bob. The polarized photon visibility is as shown in Fig. 3, the noise floor and the fiber losses are introduced into the system. However, the levels of the detected signals are sufficient to form the random codes (0 or 1). For long distance link, the problem of the entangled photon walk-off effects is occurred, whereas the compensation to obtain the optimal entangled photon states is required [10].

4. Conclusion

In conclusion, we have demonstrated the use of our scheme which is consisted of a fiber ring resonator incorporating the add/drop device as shown in Fig. 2, where the generation of noisy chaotic signal and polarized photon is achieved. The results obtained have shown that the quantum codes (qubits) can be formed. The chaotic signal is cancelled by using the appropriate add/drop device, whereas the original signal is recovered. The entangled states can be formed and is suitable for communication security, which means the use of the double security is plausible, i.e. quantum–chaotic codes can be realized and implemented in communication network. In practice, Alice and Bob can confirm the receiving states where they know the correct codes of the secret information.

Acknowledgments

The authors would like to acknowledge the Department of Applied Physics, Faculty of Science, King Mongkut's Institute of Technology Ladkrabang (KMITL) and Mahanakorn University of Technology (MUT), Thailand for supporting the laboratory facilities.

References

[1] P.P. Yupapin, W. Suwanchareon, S. Suchat, Nonlinearity penalties and benefits of light traveling in a fiber optic ring resonator, Intl. J. Light Electron Opt. 120 (2009) 216–221.
[2] S. Mitatha, K. Dejhan, P.P. Yupapin, N. Pornsuwancharoen, Chaotic signal generation and coding using a nonlinear micro ring resonator, Intl. J. Light Electron Opt. 2009, in press, doi:10.1016/j.ijleo.2008.05.028.
[3] P.P. Yupapin, W. Suwancharoen, Chaotic signal generation and cancellation using a micro ring resonator incorporating an optical add/drop multiplexer, Opt. Commun. 280/2 (2007) 343–350.
[4] P.P. Yupapin, S. Suchat, Entangle photon generation using fiber optic Mach-Zehnder interferometer incorporating the nonlinear effect in a fiber ring resonator, J. Nanophot. 1 (2007) 13504.
[5] P.P. Yupapin, W. Khunnam, S. Suchat, The entangled photons generation system using weak light in fiber optic and timing-walk off compensation, Intl. J. Quant. Inf. 5 (6) (2007) 805–814.
[6] P.P. Yupapin, P. Chunpang, A quantum–chaotic encoding system using an erbium-doped fiber amplifier in a fiber

Please cite this article as: P. Chunpang, et al., An investigation of quantum–chaotic signals generation using a fiber ring resonator and an add/drop multiplexer, Opt. Int. J. Light Electron. Opt. (2009), doi:10.1016/j.ijleo.2008.09.023

ring resonator, Intl. J. Light Electron Opt. 2009, in press, doi:10.1016/j.ijleo.2008.03.033.

[7] S. Mitatha, K. Dejhan, P.P. Yupapin, N. Pornsuwancharoen, High capacity and security packet switching using the nonlinear effects in micro ring resonator, Intl. J. Light Electron Opt. 2009, in press, doi:10.1016/j.ijleo.2008.05.032.

[8] S. Suchat, W. Khunnam, P.P. Yupapin, Entangled photon state recovery using a fiber ring resonator incorporating an erbium-doped fiber amplifier, Opt. Eng. 47 (6) (2008), 100502-1-5.

[9] P.P. Yupapin, P. Saeung, C. Li, Characteristics of complementary ring resonator add/drop filters modeling by using graphical approach, Opt. Commun. 272 (2007) 81–86.

[10] P. Trojek, Ch. Schmid, M. Bourennane, H. Weinfurter, Compact source for polarization entangled photon pairs, Opt. Express 12 (2004) 276–281.

BIOGRAPHY

Name	Mr. Phubet Phiphithirankarn
Address	99/1, Moo 11, Phoniyom Road, Muang District, Udonthani, Thailand 41000
Education	B.Sc. (Hons.) Physics, Srinakarinwirot University M.Sc. Applied Physics, King Mongkut's Institute of Technology Ladkrabang
Working Experience	2002 – 2007, Lecturer, Department of Physics, Siam University 2003 – 2004, Lecturer, Division of Physics, Udonthani Rajabhat University
Teaching Experience	Introduction to Physics Microprocessor Systems Applied Programming
Research Interests	Fiber Optic Sensors Nonlinear Fiber Optics Quantum Optics